RESEARCH MEMORANDUM

ANALYSIS OF SEVERAL METHODS OF PUMPING COOLING AIR FOR TURBOJET-ENGINE AFTERBURNERS

By John C. Samuels and Herbert Yanowitz

Lewis Flight Propulsion Laboratory
Cleveland, Ohio

NATIONAL ADVISORY COMMITTEE
FOR AERONAUTICS

WASHINGTON

February 2, 1953

NATIONAL ADVISORY COMMITTEE FOR AERONAUTICS

RESEARCH MEMORANDUM

ANALYSIS OF SEVERAL METHODS OF PUMPING COOLING AIR FOR TURBOJET-ENGINE AFTERBURNERS

By John C. Samuels and Herbert Yanowitz

SUMMARY

Several methods of pumping air to an annular cooling passage surrounding a typical axial-flow turbojet-engine afterburner were evaluated and compared on the basis of thrust and specific fuel consumption of the propulsive systems. Each of the systems was analyzed over a range of afterburner-wall temperatures, flight Mach numbers, and afterburner gas temperatures at altitudes of sea level and 35,000 feet. A typical turbojet-engine and cooling-air-passage configuration was used for the analysis.

From the viewpoint of simplicity, as well as thrust and specific fuel consumption considerations, ram pressure recovery, boundary-layer pressure recovery, and ejector systems appeared to be very satisfactory systems at high Mach numbers. At low Mach numbers, choking of the cooling passage limited the cooling-air weight flow obtainable with these systems and, therefore, the lowest attainable wall temperatures. Cooling with compressor-exit air bleed was found to be unsatisfactory because of high thrust losses, but the use of compressor bleed air as the primary fluid in a high-performance ejector was satisfactory. The use of an auxiliary compressor driven from the engine shaft increased the thrust and decreased the specific fuel consumption of the engine for many of the conditions investigated.

INTRODUCTION

Afterburning is well established as an effective means of increasing the thrust of a turbojet engine. In order to obtain the maximum thrust from an afterburner, it is necessary to burn to the highest temperatures possible (reference 1). At these high temperatures, material limitations (reference 2) necessitate the installation of cooling systems to permit safe and reliable operation.

Various methods have been proposed for cooling the afterburner wall (references 3 to 8). One of the proposed methods is cooling by means of convective heat transfer to air flowing through an annular passage surrounding the afterburner as described in reference 8. This cooling method is the one considered in this report. Both experiment and analysis (references 9 to 11) show that this method can provide satisfactory cooling for the afterburner wall. An analytical method is developed in reference 9 for calculating the maximum wall temperature of an afterburner cooled by air or gas flowing through a surrounding annular passage and the cooling-air weight flow required to maintain this temperature.

Selection of this method of afterburner cooling leads to the question of what thrust and specific fuel consumption penalties are incurred by pumping the cooling air over the burner. In order to provide this information, an analytical study was undertaken to determine the performance characteristics of several methods of pumping cooling air through a particular annular passage surrounding a typical turbojet afterburner. The methods considered in the analysis were: (a) ram or boundary-layer pressure, (b) engine-jet actuated ejector, (c) auxiliary compressor driven from the engine shaft, (d) compressor-exit air bleed, and (e) compressor-exit bleed-air actuated ejector. Each system was analyzed over a range of afterburner exhaust-gas temperatures, afterburner-wall temperatures, and flight Mach numbers at altitudes of sea level and 35,000 feet. Results of the analysis indicate the thrust and specific fuel consumption variations and the operating limits of each system when used with the jet engine and cooling passage selected for the analysis.

COOLING PASSAGE AND PUMPING TECHNIQUES

The engine used in this analysis was a typical axial-flow engine with a compressor pressure ratio of 5.20. The limiting turbine-outlet temperature was 1735° R and the assumed sea-level air flow was 93.1 pounds per second.

The cooling system selected consisted of an annular passage surrounding the afterburner wall. Air was assumed to pass through the annulus and cool the wall by means of forced convection. The cooling-air passage had an inside diameter of 32 inches, a length of 60 inches, and a height of 1/2 inch. The cooling air was pumped through the passage by the following methods: (a) ram or boundary-layer pressure recovery, (b) engine-jet actuated ejector, (c) auxiliary compressor driven from the engine shaft, (d) compressor-exit air bleed, and (e) compressor-exit bleed-air actuated ejector.

Ram and boundary-layer pressure. - For the case where the cooling air is pumped by means of ram or boundary-layer pressure recovery, the cooling air is ducted directly from a ram-air inlet or boundary-layer scoop to the cooling-air passage (fig. 1(a)). After passing through the cooling passage, the air is discharged at ambient static pressure through a variable-area nozzle. The cooling-air mass flow is controlled by this nozzle up to the point where the cooling passage chokes. Once the passage has choked the only way to increase the mass flow of cooling air is to increase the cooling-air stagnation pressure. Consequently, choking of the cooling passage limits the minimum temperatures attainable by the use of ram or boundary-layer pressure recovery.

Engine-jet actuated ejector. - The engine-jet actuated ejector (fig. 1(b)) is a simple mechanical device which uses the main jet to pump the cooling air. The cooling air from a ram or boundary-layer inlet is ducted to the cooling passage and sucked over the afterburner wall by the entraining action of the engine jet. As is the case with ram and boundary-layer pressure recovery, the lowest wall temperature obtainable at any Mach number is limited by choking of the cooling passage. The engine-jet actuated ejector considered in this report was an infinitely variable ejector. The spacing and diameter were varied to give the optimum performance at each point.

Auxiliary compressor driven from the engine shaft. - For the case of the auxiliary compressor (fig. 1(c)), a compressor with an assumed constant efficiency of 85 percent delivers air to the cooling-air passage at whatever weight flow is required. The air is supplied by either ram or boundary-layer inlets, is pumped through the cooling passage, and is then discharged to ambient pressure. The energy to run the compressor is supplied by gearing the compressor to the engine shaft. It has been estimated that a compressor that weighs less than 5 percent of the weight of the engine could maintain an afterburner-wall temperature of 1650° R with the 3900° R burner over the range of flight Mach numbers investigated at sea level.

Compressor air bleed. - For compressor air-bleed cooling (fig. 1(d)), air is bled directly from the compressor exit, ducted to the cooling passage, and discharged at the end of the cooling passage to ambient pressure. This air is under high pressure and is therefore capable of forcing itself through the cooling-air passage. The most effective way to employ compressor air bleed for cooling is to bleed off from that stage of the compressor where the air pressure is just sufficient to force the required cooling air through the passage. This method would require a complicated system of controls and was not considered in this analysis.

Compressor bleed-air actuated ejector. - A constant-area mixing ejector of the type discussed in references 12 and 13 with a diffuser added at the end of the mixing tube (fig. 1(e)) is used to pump air to the cooling-air passage. The primary fluid is supplied by bleeding air from the compressor exit and the ejector-secondary fluid is either ram or boundary-layer air.

ANALYTICAL TECHNIQUE

The analysis outlined in the following paragraphs describes the methods used to determine the flow characteristics of the cooling-air passage, the characteristics of the various pumping techniques, and the effects that extracting power has on the primary engine performance. The fuel consumption and the combined thrust of the engine and cooling-air system are then computed. Analytical and empirical methods of determining most of the information desired have been previously published and no new experimental data were required.

Determination of wall temperature. - A method for determining the maximum average wall temperature for an afterburner cooled by air passing through a surrounding annular passage has been developed in reference 9. This was accomplished by making several simplifying assumptions regarding the nature of the flow in the combustion chamber and cooling-air passage. By the method of reference 9, the exit temperature of the cooling air, which is needed to determine the wall temperature, is obtained from

$$\frac{T_{g,4} - T_{c,4}}{T_{g,4} - T_{g,3}} = \frac{1 - \left[1 - \frac{T_{g,3} - T_{c,3}}{T_{g,4} - T_{g,3}}\left(\frac{lU}{bG_c c_{p,c}}\right)\right] e^{-\frac{lU}{bG_c c_{p,c}}}}{\frac{lU}{bG_c c_{p,c}}} \tag{1}$$

All symbols are defined in appendix A. In equation (1) the dependence of the parameter $lU/bG_c c_{p,c}$ on the significant variables was determined by dimensional analysis and is the reciprocal of the following expression:

$$\frac{bG_c c_{p,c}}{lU} = 50{,}000 \left(\frac{G_c}{G_g}\right)^{0.84} \left(G_g{}^{0.29}\right)\left(\frac{b^{1.20}}{l}\right)\left(\frac{1}{T_{g,4}}\right)^{0.38} \left(\frac{1}{T_{c,3}}\right)^{0.23} \tag{2}$$

where G_c, G_g, b, l, $T_{g,4}$, and $T_{c,3}$ are specified quantities. After the cooling-air exit temperature is determined, the maximum wall temperature can be obtained from a heat balance between the hot tail-pipe gases and the cooling air at the exit of the cooling-air passage.

Typical results of the application of the preceding methods to the afterburner used in this analysis are shown in figure 2. These results are worked out for static sea-level operation of the engine. Shown also in figure 2 are results from a correlation of experimental data (reference 10) taken on a burner $60\frac{9}{16}$ inches in length and 26 inches in

[redacted]

diameter with a 1/2-inch cooling passage. These results show that the absolute values of the cooling-air requirements determined by the method of reference 9 are reasonably close to the values obtained experimentally. The theoretical method of computing cooling-air requirements was used throughout the study because it permitted investigation of a greater range of variables.

When the analytical method of reference 9 is used and a range of values for $T_{c,3}$ and λ are chosen, figure 3 can be constructed. Figure 3(a) shows the variation of afterburner-wall temperature with cooling-air inlet temperature for several values of cooling-air weight-flow ratio λ for the particular afterburner of this study. Figure 3(b) shows similar results for the cooling-air outlet temperature. It should be noted that these results are dependent on flight conditions and the afterburner-gas exit temperature. Graphs similar to figure 3 were used in the calculations for all the cooling-air pumping methods studied.

Determination of pressure drop in afterburner shroud. - Several methods exist for determining the pressure drop of fluids flowing through pipes and annuli with friction and heat addition (references 14 to 16). In this study the method of reference 16 is used because of its special reference to annular afterburner coolers. The method is based on the assumption that the longitudinal temperature distribution in the cooling-air passage may be approximated by exponential arcs. By the use of this method, the pressure drops can be computed quickly with a fair degree of accuracy.

The cooling-passage characteristics shown in figures 4 and 5 were computed from the method presented in reference 16 and from the wall temperatures shown in figure 3. In figure 4, the pumping characteristics of the passage for a typical set of conditions are given. The cooling-air outlet pressure is presented as a function of the cooling-air inlet temperature for different cooling-air weight-flow ratios at sea-level static conditions in figure 5. These figures are valid only for those operating conditions for which the cooling air is discharged directly to ambient (altitude) pressure; that is, they are used in all matching problems except those of the engine-jet actuated ejector.

Characteristics of cooling-air pumps. - In order to analyze the various cooling-air pumps, it is necessary to first determine the required cooling-air weight flow with each system for a given wall temperature over a range of flight conditions and exhaust-gas temperatures. With these values known, the conditions of the cooling air at the end of the cooling passage are determined. Knowledge of the weight flow and the exit conditions of the cooling air permits determination of the thrust or drag of the cooling air and the effect that pumping the cooling

air has on the engine performance. The evaluation of the different cooling schemes is based on two parameters: (a) the ratio of the corrected net thrust of the engine and afterburner with the cooling scheme to that without the cooling scheme, designated hereinafter as thrust ratio, and (b) the ratio of the over-all specific fuel consumption of the engine and afterburner with the cooling scheme to that without the cooling scheme, designated hereinafter as specific fuel consumption ratio. The method of computing thrust ratio and specific fuel consumption for each of the pumping schemes is given in the succeeding paragraphs. The range of variables investigated is shown in the following table:

Altitude (ft)	M_0	$T_{g,4}$ (°R)	T_w (°R)
Sea level	0 .5 .9	3500 and 3900	1500 to 2300
35,000	0.8 1.94 2.0		

Ram and boundary-layer pressure recovery. - The first step in the analysis of ram and boundary-layer pressure recovery as a cooling-air pump is to determine the conditions of the cooling air at the beginning of the cooling passage. The total temperature is determined from the well known relation

$$\frac{T_{c,5}}{t_a} = 1 + \frac{\gamma-1}{2} M_0^2 \tag{3}$$

and the total pressure is found from figure 6. The boundary-layer curve in figure 6 represents data obtained in the NACA Lewis 8- by 6-foot supersonic wind tunnel for a representative side inlet boundary-layer scoop and the ram-pressure-recovery curve represents the pressure recovery that should be attainable from an efficient practical diffuser. Equation (3) and figure 6 are used throughout this report to determine temperature and pressure recovery, respectively, as functions of flight Mach number.

From graphs similar to figure 3(a), the cooling-air weight-flow ratio is obtained from given values of flight Mach number, afterburner-wall temperature, exhaust-gas temperature, cooling-air inlet temperature, and altitude. With $T_{c,3}$, $T_{g,3}$, $T_{g,4}$, p_a, and λ known, $T_{c,4}$ is read from figure 3(b), and $T_{c,4}/t_a$ is computed. The method of reference 16 is then used to calculate $P_{c,4}/p_a$. With these values known, the thrust ratio may then be determined from the following equation:

$$\left(\frac{F_{n,c}}{F_n}\right)_E = 1 + \frac{\lambda\left(\frac{F_{j,c}}{w_c\sqrt{\theta_1}} - \frac{u_0}{g\sqrt{\theta_1}}\right)}{\left(\frac{F_n}{u_a\sqrt{\theta_1}}\right)_E} \tag{4}$$

where, for a choked passage

$$\frac{F_{j,c}}{w_c\sqrt{\theta_1}} = \sqrt{\frac{519\,\gamma R}{g}}\left\{\left(\frac{2}{\gamma-1}\,\frac{T_{c,4}}{T_1}\right)\left[1 - \left(\frac{p_a}{P_{c,4}}\right)^{\frac{\gamma-1}{\gamma}}\right]\right\}^{1/2} \tag{5}$$

and for an unchoked passage

$$\frac{F_{j,c}}{w_c\sqrt{\theta_1}} = \sqrt{\frac{519\,\gamma R}{g}}\left(\frac{1}{\gamma}\right)\left(\frac{\gamma+1}{2}\right)^{\frac{\gamma+1}{2(\gamma-1)}}\left(\frac{T_{c,4}}{T_1}\right)^{1/2}\left[\frac{2}{\left(\frac{\gamma+1}{2}\right)^{\frac{1}{\gamma-1}}} - \frac{p_a}{P_{c,4}}\right] \tag{6}$$

Since the use of boundary-layer or ram air alone does not affect the engine operation, the fuel-air ratio will not change and the specific fuel consumption ratio will be the reciprocal of the thrust ratio.

Engine-jet actuated ejector. - Because of the difficulties involved, no adequate analysis of the engine-jet actuated ejector has been made, and it was necessary to use unpublished data on a cylindrical ejector in addition to the data of references 17 to 20 in order to select the proper ejector for each flight condition. Typical experimental pumping and thrust characteristics of the engine-jet actuated ejector are shown in figures 7 and 8, respectively. The operating points of the cooling-air passage and the jet ejector for various wall temperatures and flight conditions are fixed by determining a configuration which gives the required pumping for the specified wall temperature while at the same time producing the maximum thrust obtainable for that cooling-air flow. Experimental ejector thrust and pumping charts such as shown in figures 7 and 8 are used in this matching process.

The first step in the matching process is to determine the state of the air entering the cooling passage by the use of equation (3) and figure 6. From figure 3(a), the cooling-air weight-flow ratio is obtained from the given values of M_0, t_a, $T_{g,3}$, $T_{c,3}$, and p_a. With these values known, $T_{c,4}$ is read from figure 3(b), and $P_{c,4}/p_a$ is computed by the methods of reference 16. From engine-cycle analysis, $P_{g,4}/p_a$ is

computed and an ejector configuration is selected to give the maximum thrust ratio for particular values of $P_{c,4}/p_a$, $P_{g,4}/p_a$, and $\lambda\sqrt{T_{c,4}/T_{g,4}}$. Because the primary nozzle was operated choked at all points, the ejector did not affect the operation of the engine and the specific fuel consumption ratio is the reciprocal of the thrust ratio.

The data presented in references 17 to 20 are for gases at room temperature, and performance data obtained with hot gases may be different. The square root of the temperature ratio $T_{c,4}/T_{g,4}$ will tend to correct the ejector weight-flow ratio to that of room temperature (reference 22), and therefore this correction was used. Since no report shows that the thrust of an ejector is considerably affected by temperature, no correction was applied to the thrust data presented in references 17 to 20.

Auxiliary compressor driven from engine shaft. - As in the two previous cases, the state of the cooling air at the inlet to the compressor is determined by means of equation (3) and figure 6. Also required in the matching problem is the relation between the pressure ratio and the temperature ratio of the auxiliary compressor. The compressor performance used herein, which is shown in figure 9, was computed from the following expression:

$$\frac{P_{c,3}}{P_5} = \left[1 + \eta\left(\frac{T_{c,3}}{T_5} - 1\right)\right]^{\frac{\gamma}{\gamma-1}} \tag{7}$$

It was assumed that the compressor could deliver any quantity of air at the desired pressure ratio with a constant efficiency of 85 percent.

The operating points of the cooling-air passage and the auxiliary compressor can be determined from the location of the intersections of the passage characteristics (fig. 4) and the compressor characteristics (fig. 9). Before this determination is made, the pressure-ratio scale of the auxiliary compressor characteristics curve must be multiplied by the ram or boundary-layer pressure-recovery ratio and the temperature-ratio scale must be multiplied by $1 + \frac{\gamma-1}{2} M_0^2$. In figure 4, the auxiliary fan characteristics are superimposed over the passage characteristics for sea-level static operation and an exhaust-gas temperature of 3500° R. If a value of λ is chosen, values of $T_{c,3}/t_a$ and $P_{c,3}/p_a$ can be determined from the intersection of the two curves. With the value of $T_{c,3}/t_a$ known, $T_{c,3}$, $T_{c,4}$, T_w, and $P_{c,4}$ may be determined. The selection of a range of values for λ permits a range of values for T_w to be investigated at each flight condition.

In order to determine the thrust and specific fuel consumption ratios, the effect of extracting energy from the engine shaft must be known in addition to the thrust provided by the cooling air. Figure 10 was constructed using the methods of reference 21. This figure shows the variation of the thrust ratio with the power extraction factor. These curves do not include the effects of cooling-air thrust and are good only for an exhaust-gas temperature of 3900° R. Similar curves were prepared for an exhaust-gas temperature of 3500° R. (The value of thrust ratio without cooling-air thrust is read from these charts using the value of the power extraction factor at the match point.) The thrust ratio of the cooling air is added to this and the over-all thrust ratio is obtained from

$$\left(\frac{F_{n,c}}{F_n}\right)_E = \left(\frac{F_{n,c}}{F_n}\right)_P + \frac{\lambda\left(\frac{F_{j,c}}{w_c\sqrt{\theta_1}} - \frac{u_0}{g\sqrt{\theta_1}}\right)}{\left(\frac{F_n}{w_a\sqrt{\theta_1}}\right)_E} \tag{8}$$

The specific fuel consumption ratio with cooling is obtained by dividing the sum of the engine fuel, as determined from the method of reference 21, and the afterburner fuel flow by the thrust of the afterburner and cooling-air jet. The afterburner fuel flow is determined by the application of an enthalpy balance to the afterburner. The combustion efficiency of the primary combustor was assumed to be 0.98 and that of the afterburner, 0.95. The specific fuel consumption of the propulsive system with cooling is divided by the specific fuel consumption without cooling to obtain the specific fuel consumption ratio.

Compressor-air bleed cooling. - For a given bleed ratio and flight condition, the engine compressor temperature and pressure ratios may be computed from results reported in reference 22. Typical results used in this analysis are shown in figure 11. The results of this particular figure are for static sea-level operation of the engine. Figure 12 was constructed from the results of reference 22 and shows the effect of the bleed ratio β on the thrust ratio without cooling-air thrust added for an exhaust-gas temperature of 3900° R at sea level.

In order to determine the state of the cooling air at the entrance to the cooling-air passage, a bleed ratio and flight condition must first be specified so that the pressure and the temperature can be read from compressor-performance figures similar to figure 11. With these values known, T_w, $P_{c,4}$, and $T_{c,4}$ can be found and the thrust and the specific fuel consumption ratios determined.

[redacted]

The thrust ratio is determined by first using the chosen value of β and figure 12 to determine the thrust ratio without thrust recovery from the cooling air. To this is added the thrust ratio of the cooling air. The thrust ratio is given by

$$\left(\frac{F_{n,c}}{F_n}\right)_E = \left(\frac{F_{n,c}}{F_n}\right)_\beta + \frac{\beta\left(\frac{F_{j,c}}{w_c\sqrt{\theta_1}}\right)}{\left(\frac{F_n}{w_a\sqrt{\theta_1}}\right)_E} \tag{9}$$

The specific fuel consumption ratio is the quotient of the over-all specific fuel consumption with cooling and the over-all specific fuel consumption without cooling. The engine fuel flow with compressor bleed is calculated by the method used in reference 22.

Compressor bleed-air actuated ejector. - The pumping characteristics of this ejector are shown in figure 13. (See appendix B for the derivation of the equations from which fig. 13 is computed.) It should be noted that along each curve in this figure the weight-flow ratio and the ejector geometry are varying continuously. The first step in the matching problem is to determine the stagnation state of the ejector primary fluid for a given bleed ratio from figure 11. The state of the secondary air is determined from figure 6 and equation (3). An operating point of the passage and the compressor bleed-air actuated ejector is obtained when M_0, p_a, λ, and β are specified. The parameters σ and τ are determined when M_0, p_a, and β are given. The ejector temperature ratio is obtained from

$$\frac{T_{c,3}}{T_5} = \frac{\tau + \omega}{1 + \omega} = \frac{\tau + \frac{\lambda - \beta}{\beta}}{1 + \frac{\lambda - \beta}{\beta}} \tag{10}$$

With $T_{c,3}/T_5$, σ, and τ known, the ejector pressure ratio is read from figure 13. The wall temperature and the cooling-air exit temperature are determined from figure 3, and $P_{c,4}$ is then computed by the methods of reference 16.

With these parameters known, the thrust ratio can be determined. The thrust ratio without thrust recovery from the cooling air is determined by using the chosen value of β and figure 12. To this is added the thrust ratio of cooling air. The thrust ratio is given by

$$\left(\frac{F_{n,c}}{F_n}\right)_E = \left(\frac{F_{n,c}}{F_n}\right)_\beta + \frac{\lambda\left(\frac{F_{j,c}}{w_a\sqrt{\theta_1}} - \frac{\lambda - \beta}{\lambda}\frac{V_0}{g\sqrt{\theta_1}}\right)}{\left(\frac{F_n}{w_a\sqrt{\theta_1}}\right)_E} \tag{11}$$

[redacted]

The specific fuel consumption ratio is determined in the same manner used for the case in which compressor bleed-air cooled the afterburner.

PERFORMANCE RESULTS

The performance of the engine with the various cooling-air pumping methods is presented in terms of thrust and specific fuel consumption ratios as functions of the afterburner-wall temperature. The engine was assumed to be operating at rated speed and limiting turbine-outlet temperature at all times.

Ram and boundary-layer air cooling. - The performance of the engine with ram and boundary-layer air cooling is shown in figures 14 to 17. At the higher afterburner-wall temperatures, the performance of the engine is virtually unaffected by cooling with ram or boundary-layer air. However, the wall temperatures obtainable with these techniques are severely limited by choking of the cooling-air passage. The lowest wall temperature obtainable with the high-temperature burner (3900° R) was 1925° R and occurred at a flight Mach number of 2.0 using ram air as coolant (fig. 14(a)); but when boundary-layer air was used, the lowest wall temperature obtainable was 2010° R and occurred at a flight Mach number of 0.90 (fig. 16(a)). A minimum wall temperature of 1695° R was obtained with the 3500° R burner using ram air as coolant (fig. 14(b)), while a minimum temperature of 1760° R was obtained with boundary-layer air. Gas temperature and flight Mach number had practically no effect on the thrust and specific fuel consumption ratios of the engine in these cases, but flight Mach number was found to have a direct bearing on the lowest wall temperatures obtainable (figs. 14 to 17).

Engine-jet actuated ejector. - The performance of the engine and afterburner using the jet ejector with ram air as a cooling-air pump is shown in figures 18 and 19. It should be noted that each curve in figures 18 and 19 begins with that wall temperature for which the passage is choked. As a result of this choking of the cooling-air passage, the engine-jet actuated ejector can not maintain afterburner-wall temperatures below 1925° R with the 3900° R burner, or below 1695° R with the 3500° R burner, at any of the flight conditions investigated. Whenever the jet ejector is usable as a cooling-air pump, thrust ratios above 1 and specific fuel consumption ratios below 1 are obtained at the high flight Mach numbers. This is primarily due to the similarity of ejector behavior with that of a convergent-divergent nozzle (reference 23), and thus the thrust ratio parameter essentially compares the thrust of a convergent-divergent nozzle with the thrust of a convergent nozzle. Because of the very slight difference (less than 2 percent) in performance of the jet ejector using boundary-layer air as compared with ram air, only the curves for the ejector using ram air are shown.

Auxiliary compressor driven from engine shaft. - The performance of the engine geared to an auxiliary compressor which pumps ram air to the cooling passage is presented in figures 20 to 23. It is interesting to note that, as a result of an increase in the thrust of the cooling air, a decrease in wall temperature generally corresponds to an increase in the thrust ratio and a decrease in the specific fuel consumption ratio. Consequently, over a large range of flight conditions the auxiliary compressor acts as a thrust augmentor as well as a cooling-air pump.

Comparison of figures 20 and 21 shows that flight Mach number and exhaust-gas temperature have only second-order effects on the thrust and specific fuel consumption ratios. The effects of different efficiencies on the performance of the propulsive system for sea-level static operation are shown in figures 22 and 23. The effect of using boundary-layer air instead of ram air was so slight that only the ram-air curves are shown.

2545

Compressor air-bleed cooling. - In figures 24 and 25 the performance of the engine with compressor bleed is shown. From these figures it can be seen that any wall temperature down to 1700° R or lower may be obtained, if desired, but at the expense of a considerable increase in the specific fuel consumption and a decrease in the thrust ratio reaching 1.16 and 0.59, respectively, for an exhaust-gas temperature of 3900° R, an afterburner-wall temperature of 1600° R, and sea-level static operation (figs. 24(a) and 25(a)). Thrust-ratio losses increased as much as 10 percent in going from an exhaust-gas temperature of 3500° to 3900° R (fig. 24).

The effect of flight Mach number on the thrust and specific fuel consumption ratios is greatest at the lower wall temperatures and with the high-temperature afterburner (figs. 24 and 25). With an exhaust-gas temperature of 3900° R at an altitude of 35,000 feet and a wall temperature of 1700° R, the change in thrust ratio and specific fuel consumption ratio over the range of Mach numbers investigated is about $7\frac{1}{2}$ percent.

Compressor bleed-air actuated ejector. - The performance of the engine with an air ejector actuated by compressor bleed air for a cooling-air pump is shown in figures 26 to 28. The air ejector is assumed to have a weight-flow ratio of 3.00. Flight Mach number has only a minor effect on thrust and specific fuel consumption ratios, particularly at the higher wall temperatures (fig. 26). It is clear that any wall temperature in the range investigated can be obtained with only moderate losses in thrust and specific fuel consumption (fig. 27). There seems to be no significant change in the performance of the engine in going from an average exhaust-gas temperature of 3500° to 3900° R when the compressor bleed-air ejector is used as a cooling-air pump. Furthermore, the difference between the thrust and specific fuel consumption ratios when boundary-layer air is used as the ejector secondary fluid instead of ram air is so slight that only the curves for ram air are shown.

[redacted]

The most efficient way to use the air ejector as a cooling-air pump is to vary the weight-flow ratio. The weight-flow ratio is then optimized for each flight condition. Because of the many variables involved in the analysis of this particular pumping combination, it was not considered practical to present curves showing the effect of various weight-flow ratios for every flight condition. The effect at sea-level static conditions of different weight-flow ratios on thrust ratio is shown in figure 28. It appears from examination of figure 28, that an increase in weight-flow ratio causes large increases in thrust ratio. Such increases in thrust ratio are possible up to the point where ejector geometry and flight conditions cause choking in the secondary passage. Once the secondary passage is choked, no further increase in weight-flow ratio or in thrust ratio is possible. The weight-flow ratio of 3.00 was chosen for this report because it gave nearly optimum performance and did not cause choking for all of the flight conditions investigated.

Comparison of Various Cooling-Air Pumping Methods

The performance of the propulsive system with the various cooling-air pumping techniques can be compared by cross plotting the results shown in figures 14 to 28. Such a comparison is made in figure 29 for an afterburner operating with an exhaust-gas temperature of 3500° R and a wall temperature of 1860° R. All the cooling schemes except that of boundary-layer pressure recovery are shown using ram air. From figures 29(a) and 29(b) it can be seen that the auxiliary compressor has a higher thrust ratio and lower specific fuel consumption ratio than all the other pumps at sea-level static operation. The thrust ratio of the auxiliary compressor at this condition is 1.015 and the specific fuel consumption ratio is 0.990. This thrust ratio of 1.015 represents an actual gain in augmented thrust as a consequence of cooling the afterburner. The auxiliary compressor, however, is inferior to ram or boundary-layer air at the high Mach numbers where either can be employed. At sea level, sufficient cooling is not supplied by ram-air cooling below a flight Mach number of 0.655 or by boundary-layer air below a Mach number of 0.752.

The performance of the engine-jet actuated ejector is poor at takeoff but improves with increasing flight Mach number, and at a Mach number of 0.79 surpasses all the other cooling schemes. Because increasing the cooling-air pressure ratio causes the jet ejector to act more like an isentropic nozzle, it appears that a combination of the engine-jet actuated ejector and the compressor-bleed-air actuated ejector or the auxiliary compressor could be used to obtain a higher thrust ratio at all flight conditions.

A comparison of the cooling schemes is shown in figures 29(c) and 29(d) for an altitude of 35,000 feet. The most important features of these curves are that boundary-layer air will not cool the afterburner wall to 1860° R in the Mach number range investigated and that the

engine-jet actuated ejector has a higher thrust ratio and a lower specific fuel consumption ratio than all the other cooling-air pumps above a flight Mach number of 1.11. Below this Mach number, the cooling-air passage is choked and the ejector cannot pump enough air to cool the afterburner shell to 1860° R. Ram-air pressure recovery is also insufficient to pump enough cooling air below a Mach number of 1.11. In order to encompass the complete range of flight conditions, the engine-jet actuated ejector could be used in series with the compressor bleed-air actuated ejector or the auxiliary compressor; these combinations would give higher thrust ratios than when any of these techniques was used alone.

CONCLUSIONS

An analysis has been made of the performance of several methods of pumping cooling air to turbojet-engine afterburners utilizing cooling-air flow requirements from previous experimental and analytical investigations. The performance of the cooling-air schemes was evaluated for various operating temperatures and flight conditions on the basis of (a) the ability to pump cooling air and (b) the effects of pumping the cooling air on the thrust and specific fuel consumption of the engine.

This analysis showed that ram and boundary-layer pressure are high enough to supply sufficient cooling air only at high flight Mach numbers. Choking limitations in the cooling-air passage limited the applicability of the engine-jet actuated ejector at low flight speeds to exhaust-gas temperatures below 3500° R. At high flight Mach numbers, however, the performance of the engine-jet actuated ejector improved because of the increased density and pressure ratio of the cooling air. Cooling with compressor-exit air bleed is unsatisfactory because of high thrust losses and specific fuel consumption increases, but the use of compressor-exit bleed air as the primary fluid in a high-performance ejector gives satisfactory performance over the entire range of flight conditions. Very good performance over the range of flight conditions can also be obtained with an auxiliary compressor geared to the engine. These results suggest that further improvements may be obtained by using the auxiliary compressor or the high-performance ejector in series with the engine-jet actuated ejector.

Lewis Flight Propulsion Laboratory
National Advisory Committee for Aeronautics
Cleveland, Ohio

[redacted]

APPENDIX A

SYMBOLS

The following symbols are used in this report.

A	area, sq ft
b	cooling-passage height, ft
c_p	specific heat at constant pressure, Btu/(lb)($^{\circ}$R)
c_v	specific heat at constant volume, Btu/(lb)($^{\circ}$R)
D	diameter, ft
F_1,F_2,F_3	factors used in ejector analysis (defined in appendix B)
$F_{j,c}$	jet thrust of cooling air, lb
F_n	net thrust, lb
$F_{n,c}$	total net thrust with cooling
G	mass velocity, lb/(sec)(sq ft)
g	acceleration due to gravity, ft/sec^2
H	enthalpy, Btu/lb
J	mechanical equivalent of heat, ft-lb/Btu
L	mixing-tube length, ft
l	cooling-passage length, ft
M	Mach number
M_O	flight Mach number
P	total pressure, lb/sq ft
p	static pressure, lb/sq ft
R	gas constant, ft-lb/(lb)($^{\circ}$R)
SFC	net thrust specific fuel consumption

[redacted]

T	total temperature, $^{\circ}R$
t	static temperature, $^{\circ}R$
U	heat-transfer coefficient, Btu/(sq ft)(sec)($^{\circ}R$)
u	velocity, ft/sec
w	weight flow, lb/sec
α	$\frac{\text{ejector mixing-tube area}}{\text{ejector primary nozzle-throat area}}$
α'	$\frac{\text{ejector primary nozzle-exit area}}{\text{ejector primary nozzle-throat area}}$
β	compressor bleed ratio
γ	c_p/c_v
ϵ	empirical factor
η	compressor efficiency
η_D	ejector diffuser efficiency
θ	$\frac{\text{total temperature}}{\text{NACA standard temperature}}$
λ	$\frac{\text{cooling-air weight flow}}{\text{engine-air weight flow}}$
σ	$\frac{\text{ejector primary total pressure}}{\text{ejector secondary total pressure}}$
τ	$\frac{\text{ejector primary total temperature}}{\text{ejector secondary total temperature}}$
ω	ejector weight-flow ratio

Subscripts:

a	air

[redacted]

c	cooling air
E	engine plus afterburner
g	gas
P	shaft power extraction
p	primary
s	secondary
w	wall
β	compressor bleed
0	free stream
1	compressor inlet
2	compressor exit
3	tail-pipe and cooling-passage entrance
4	tail-pipe and cooling-passage exit
5	cooling-passage scoop

Superscripts:

'	ejector primary stream
''	ejector secondary stream

[redacted]

APPENDIX B

ANALYSIS OF COMPRESSOR BLEED-AIR EJECTOR PUMP

The ejector shown in the schematic diagram in figure 30 may be analyzed readily if it is assumed that:

(1) The flow is one-dimensional.

(2) The flow is isentropic from station 0 to station 1.

(3) The mixing tube has a constant area

(4) The mixing-tube length is such that the primary and secondary streams are completely mixed at station 2.

(5) The diffuser has a constant efficiency.

(6) Friction effects are negligible.

With these assumptions, a balance of mass flow, momentum, and energy may be written between stations 1 and 2. They are, in order,

$$w = w' + w'' \tag{B1}$$

$$\frac{w'u_1'}{g} + p_1'A_1' + \frac{w''u_1''}{g} + p_1''A_1'' = \frac{wu_2}{g} + p_2A_2 \tag{B2}$$

$$w'H_0' + w''H_0'' = w\left(H_2 + \frac{u_2^2}{2gJ}\right) \tag{B3}$$

where ' and '' refer to the primary and secondary streams, respectively. By definition

$$\omega \equiv \frac{w''}{w'} = \left(\frac{\alpha}{\alpha'} - 1\right)\sqrt{\tau}\left(\frac{M_1''}{M_1'}\right)\left(\frac{p_0'}{p_0''}\right)^{\frac{1-\gamma}{2\gamma}} \tag{B4}$$

where it is assumed that the thermodynamic constants of the fluid are constant and that the primary nozzle is always fully expanded. From equation (B2) the following equation is obtained:

$$\frac{p_2}{p_0'}\left(1 + \gamma M_2^2\right) = \left[\left(1 + \gamma M_1'^2\right)\frac{\alpha'}{\alpha} + \left(1 + \gamma M_1''^2\right)\left(1 - \frac{\alpha'}{\alpha}\right)\right]\frac{p_1}{p_0'} \equiv F_1 \tag{B5}$$

[redacted]

where $p_1' = p_1'' = p_1$

If equations (B1) and (B4) are used, the energy equation may be written as

$$\left(\frac{p_2}{p_0'}\right)^2 \left(1 + \frac{\gamma - 1}{2} M_2^2\right) M_2^2 = \frac{(\tau + \omega)(1 + \omega)}{\tau\alpha^2} \left(\frac{2}{\gamma + 1}\right)^{\frac{\gamma+1}{\gamma-1}} \equiv F_2 \tag{B6}$$

Let $F_3 \equiv \frac{F_2}{F_1^2}$; then, the use of equations (B5) and (B6) yields the Mach number at station 2:

$$M_2^2 = -\frac{\gamma F_3 - \frac{1}{2}}{\gamma^2 F_3 - \frac{\gamma - 1}{2}} \pm \sqrt{\left(\frac{\gamma F_3 - \frac{1}{2}}{\gamma^2 F_3 - \frac{\gamma - 1}{2}}\right)^2 - \frac{F_3}{\gamma^2 F_3 - \frac{\gamma - 1}{2}}} \tag{B7}$$

Note also that

$$\frac{p_2}{p_0'} = \frac{F_1}{1 + \gamma M_2^2} \tag{B8a}$$

$$\frac{T_3}{T_0''} = \frac{\tau + \omega}{1 + \omega} \tag{B8b}$$

An analysis of the diffuser of efficiency η_D shows that the stagnation pressure at station 3 can be computed from

$$\frac{p_3}{p_0''} = \frac{p_2}{p_0'} \left(\frac{p_0'}{p_0''}\right) \left(1 + \frac{\gamma - 1}{2} \eta_D M_2^2\right)^{\frac{\gamma}{\gamma-1}} \tag{B9}$$

Thus, for given (or assumed) values of p_0'/p_0'', τ, and M_1'', the ejector temperature ratio may be determined from equation (B8b) and the pressure ratio from equation (B9). Figure 16 was constructed from the results of this analysis with $\eta_D = 0.80$, $M_1'' = 0.60$, and $A_3/A_2 = \infty$ (diffuser-area ratio).

It should be noted that equation (B4) gives the theoretical weight-flow ratio of the ejector. The actual weight-flow ratio is equal to ω where ε is less than 1 and is determined from experiment. A value of $\varepsilon = 0.90$ was used in calculating the data for figure 13. The introduction

of this empirical factor causes the computed ejector pressure ratio to be lower than the ideal and also causes the ejector temperature ratio to be higher than the ideal. It also has the effect of making only one solution of equation (B7) possible, namely, a subsonic solution.

REFERENCES

1. Lundin, Bruce T.: Theoretical Analysis of Various Thrust-Augmentation Cycles for Turbojet Engines. NACA Rep. 981, 1950. (Supersedes NACA TN 2083.)

2. Anon: Engineering Properties of Inconel. Bull. T-7, Dev. and Res. Div., The International Nickel Co., Inc. (New York), March 1943.

3. Perchonok, Eugene, Sterbentz, William H., and Wilcox, F. A.: Performance of a 20-Inch Steady-Flow Ram Jet at High Altitudes and Ram-Pressure Ratios. NACA RM E6L06, 1947.

4. Shepherd, T. L.: An Investigation of the Structure Temperatures in the Combustion Chambers of the P/A VI. Rep. No. 5662, Eng. Dept., Chance Vought Aircraft, July 21, 1947.

5. Perchonok, Eugene, Wilcox, Fred A., and Sterbentz, William H.: Investigation of the Performance of a 20-Inch Ram Jet Using Preheated Fuel. NACA RM E6I23, 1946.

6 Woodward, William H., and Bobrowsky, A. R.: Preliminary Investigation of a Ceramic Lining for a Combustion Chamber for Gas-Turbine Use. NACA RM E7H20, 1948.

7. Williams, D. T., and Dunlap, R. A.: Equilibrium Temperature of a Ram-Jet Burner Shell. External Memo No. 12, Dept. Eng. Res., Univ. Mich., Nov. 10, 1947. (AAF Contract W33-038-ac-14222, Proj. MX-794, ATI 19218.)

8. Ellerbrock, Herman H., Jr., Wcislo, Chester R., and Dexter, Howard E.: Analysis, Verification, and Application of Equations and Procedures for Design of Exhaust-Pipe Shrouds. NACA TN 1495, 1947.

9. Koffel, William K., Stampers, Eugene, and Sanders, Newell D.: Cooling of Ram Jets and Tail-Pipe Burners - Analytical Method for Determining Temperatures of Combustion Chambers Having Annular Cooling Passage. NACA RM E9L09, 1950.

10. Koffel, William K., and Kaufman, Harold R.: Empirical Cooling Correlation for an Experimental Afterburner with an Annular Cooling Passage. NACA RM E52C13, 1952.

[redacted]

11. Koffel, William K., and Kaufman, Harold R.: Investigation of Heat-Transfer Coefficients in an Afterburner. NACA RM E52D11, 1952.

12. Flügel, Gustav: The Design of Jet Pumps. NACA TM 982, 1941.

13. Keenan, J. H., and Neuman, E. P.: A Simple Air Ejector. Jour. Appl. Mech., vol. 9, no. 2, June 1942, pp. A75-A81.

14. Pinkel, Benjamin, Noyes, Robert N., and Valerino, Michael F.: Method for Determining Pressure Drop of Air Flowing Through Constant-Area Passages for Arbitrary Heat-Input Distributions. NACA TN 2186, 1950.

15. Shapiro, Ascher H., and Hawthorne, W. R.: The Mechanics and Thermodynamics of Steady One-Dimensional Gas Flow. Jour. Appl. Mech., vol. 14, no. 4, Dec. 1947, pp. A317-A336.

16. Sibulkin, Merwin, and Koffel, William K.: Charts for Simplifying Calculations of Pressure Drop of a High-Speed Compressible Fluid under Simultaneous Action of Friction and Heat Transfer - Application to Combustion-Chamber Cooling Passages. NACA TN 2067, 1950.

17. Greathouse, W. K., and Hollister, D. P.: Preliminary Air-Flow and Thrust Calibrations of Several Conical Cooling-Air Ejectors with a Primary to Secondary Temperature Ratio of 1.0. I - Diameter Ratios of 1.21 and 1.10. NACA RM E52E21, 1952.

18. Greathouse, W. K., and Hollister, D. P.: Preliminary-Air Flow and Thrust Calibrations of Several Conical Cooling-Air Ejectors with a Primary to Secondary Temperature Ratio of 1.0. II - Diameter Ratios of 1.06 and 1.40. NACA RM E52F26, 1952.

19. Kochendorfer, Fred D., and Rousso, Morris D.: Performance Characteristics of Aircraft Cooling Ejectors Having Short Cylindrical Shrouds. NACA RM E51E01, 1951.

20. Wilsted, H. D., Huddleston, S. C., and Ellis, C. W.: Effect of Temperature on Performance of Several Ejector Configurations. NACA RM E9E16, 1949.

21. Koutz, Stanley L., Hensley, Reece V., and Rom, Frank E.: Effect of Heat and Power Extraction on Turbojet-Engine Performance. III - Analytical Determination of Effects of Shaft-Power Extraction. NACA TN 2202, 1950.

22. Hensley, Reece V., Rom, Frank E., and Koutz, Stanley L.: Effect of Heat and Power Extraction on Turbojet-Engine Performance. I - Analytical Method of Performance Evaluation with Compressor-Outlet Air Bleed. NACA TN 2053, 1950.

23. Fleming, W. A.: Internal Performance of Several Types of Jet-Exit Configuration for Supersonic Turbojet Aircraft. NACA RM E52K04, 1952.

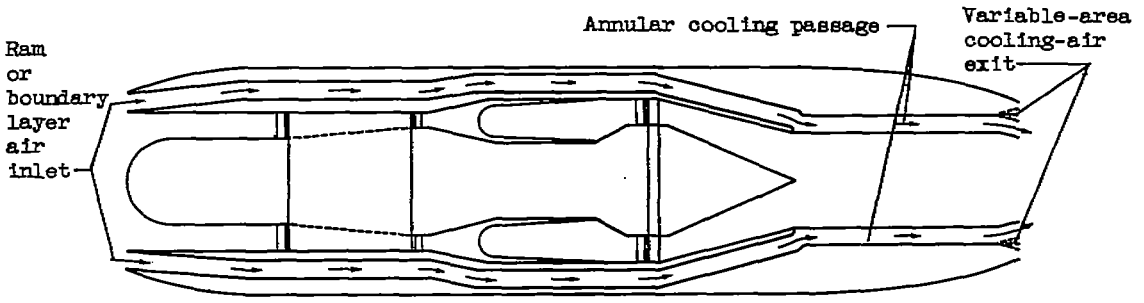

(a) Ram or boundary-layer pressure.

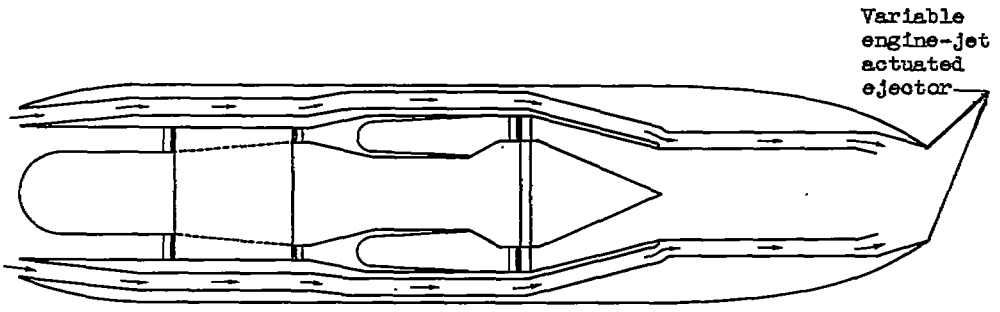

(b) Engine-jet actuated ejector.

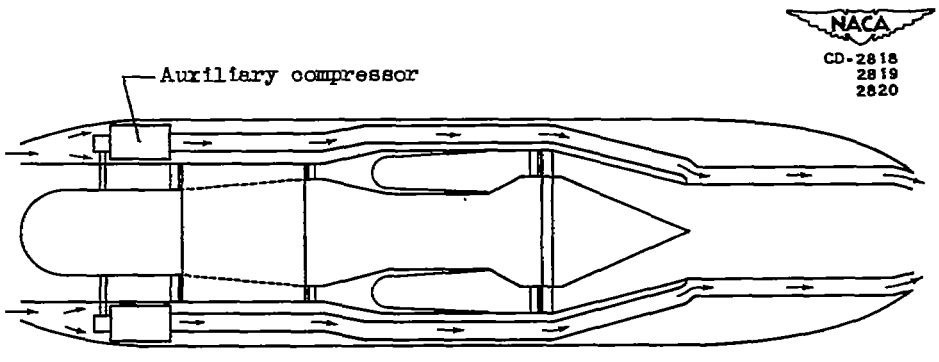

(c) Auxiliary compressor.

Figure 1. - Schematic diagrams of various cooling-air pumping methods.

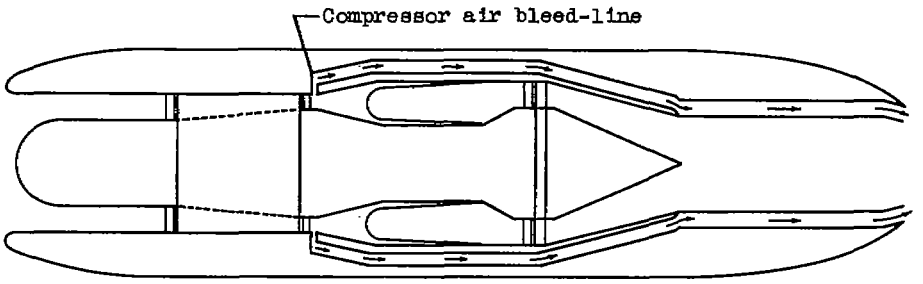

(d) Compressor air bleed.

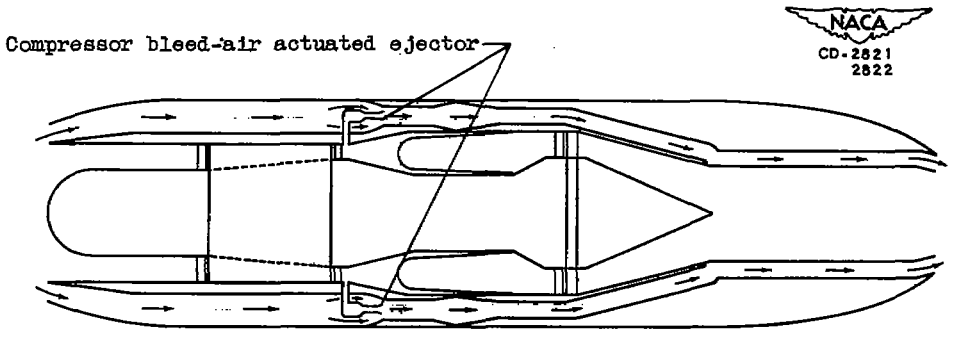

(e) Compressor bleed-air actuated ejector.

Figure 1. - Concluded. Schematic diagrams of various cooling-air pumping methods.

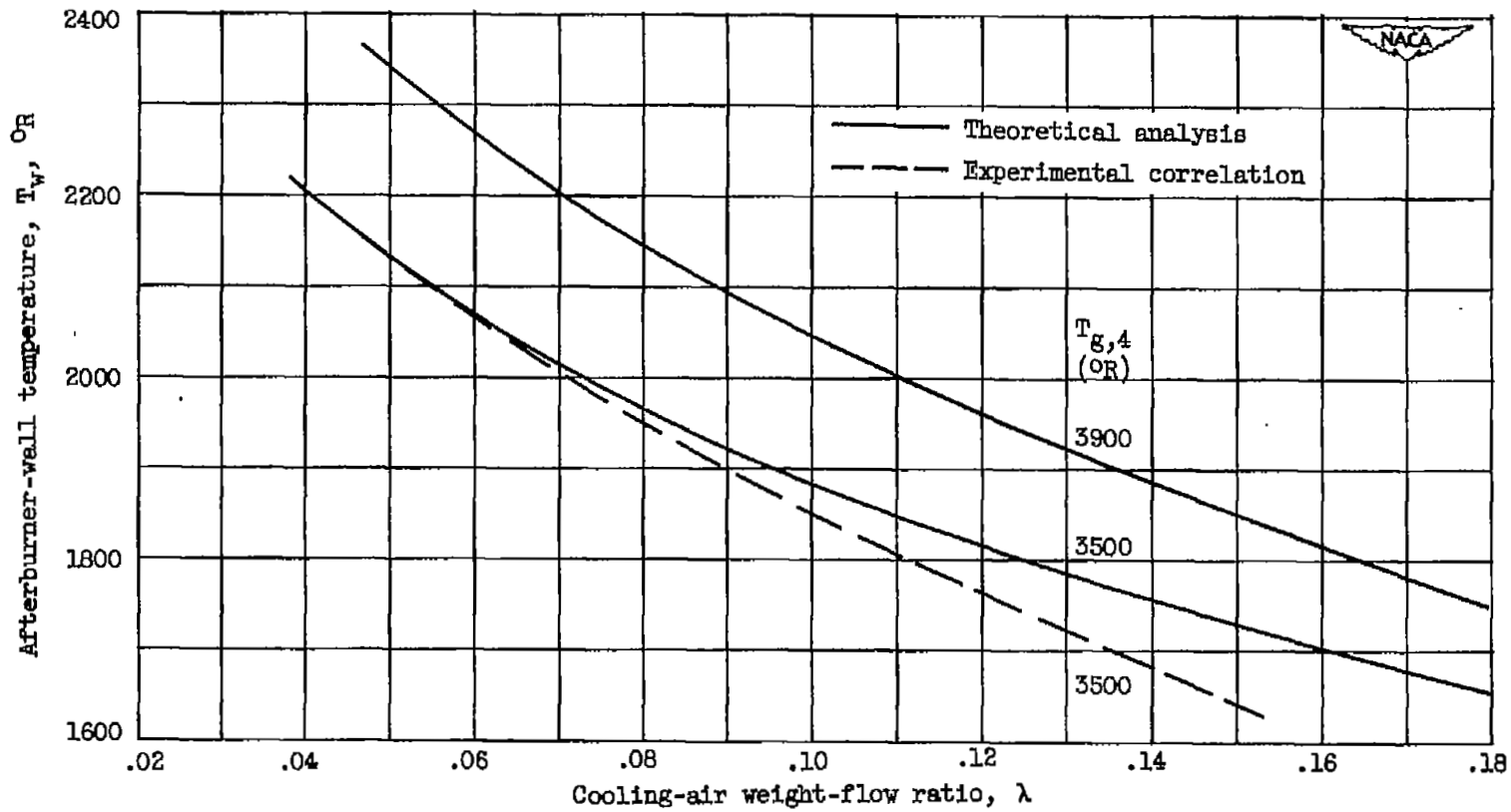

Figure 2. - Experimental and theoretical cooling-air flow requirements at sea-level conditions. Flight Mach number, 0.

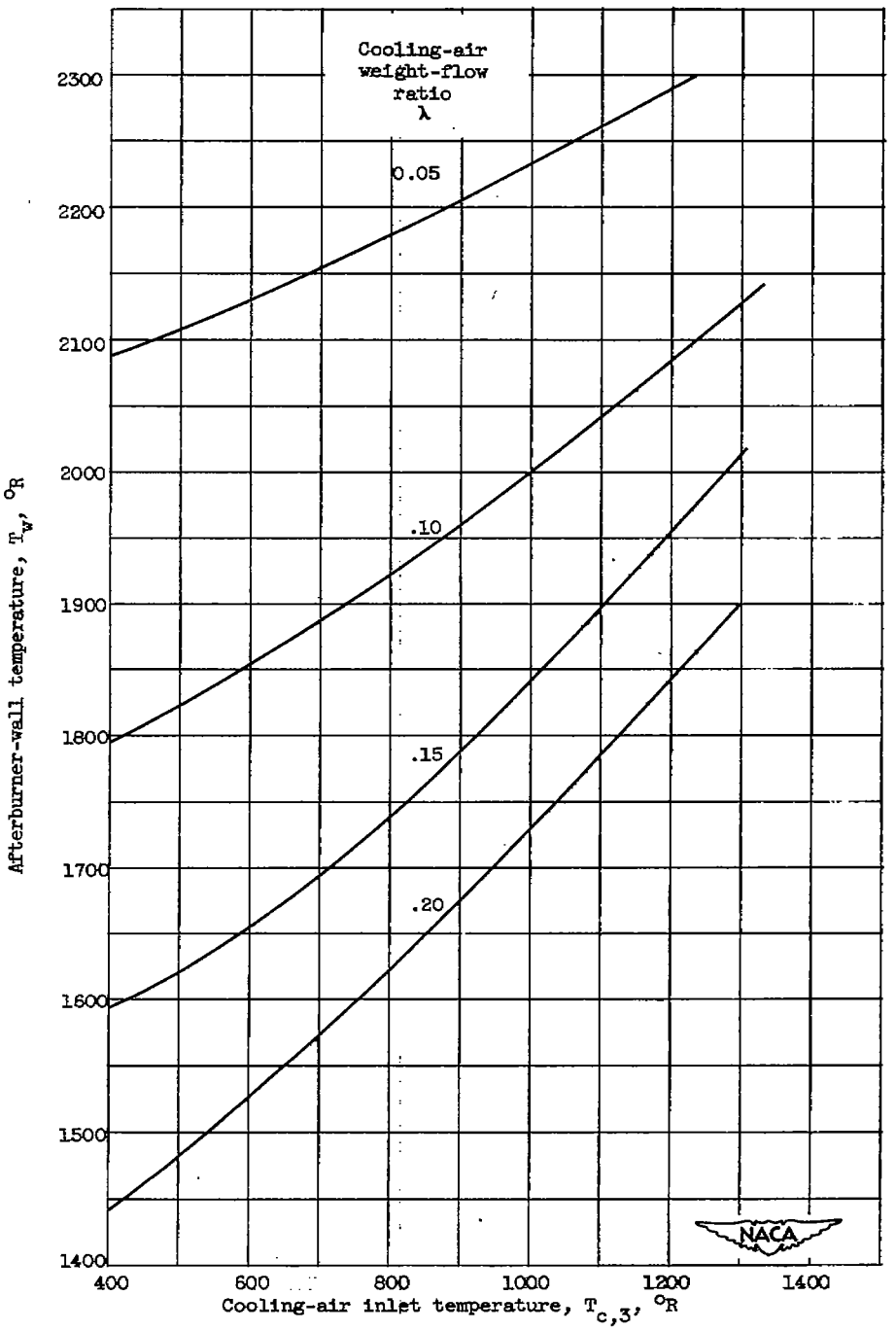

(a) Afterburner-wall temperature.

Figure 3. - Afterburner-wall temperature and cooling-air outlet temperature as a function of cooling-air inlet temperature and weight-flow ratio at sea-level conditions. Exhaust-gas temperature, 3500° R; flight Mach number, 0.

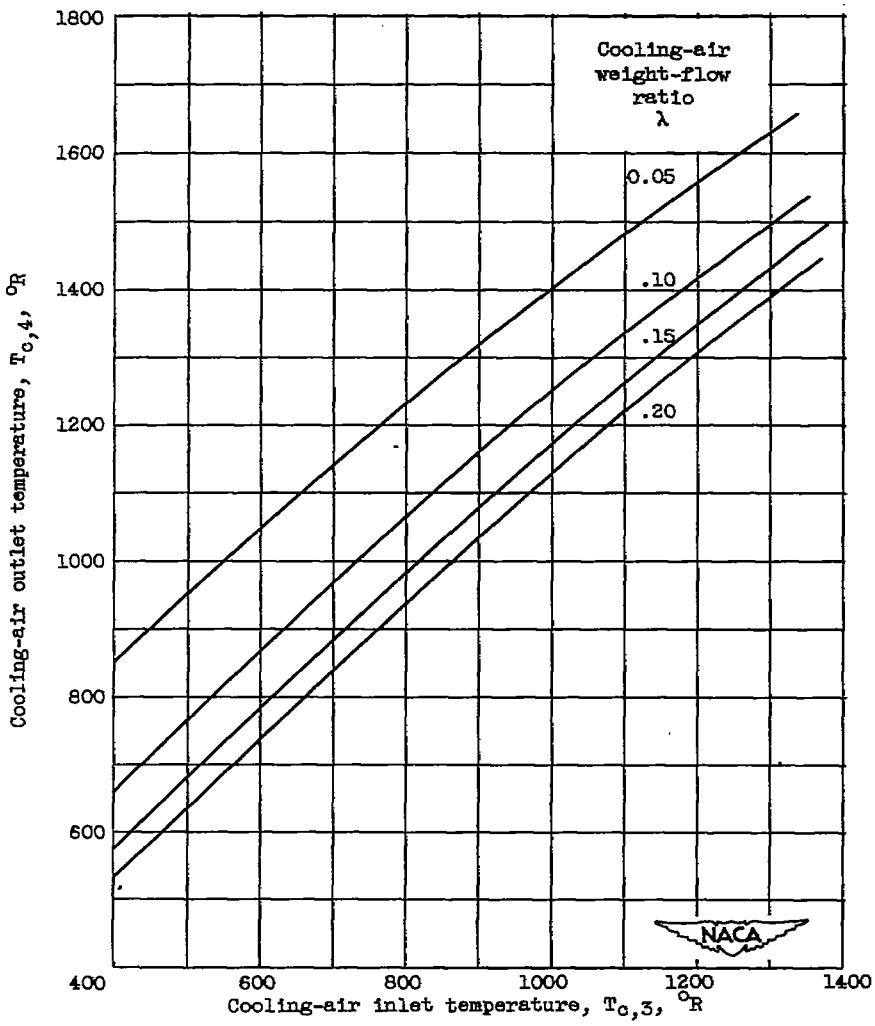

(b) Cooling-air outlet temperature.

Figure 3. - Concluded. Afterburner-wall temperature and cooling-air outlet temperature as a function of cooling-air inlet temperature and weight-flow ratio at sea-level conditions. Exhaust-gas temperature, 3500° R; flight Mach number, 0.

[redacted]

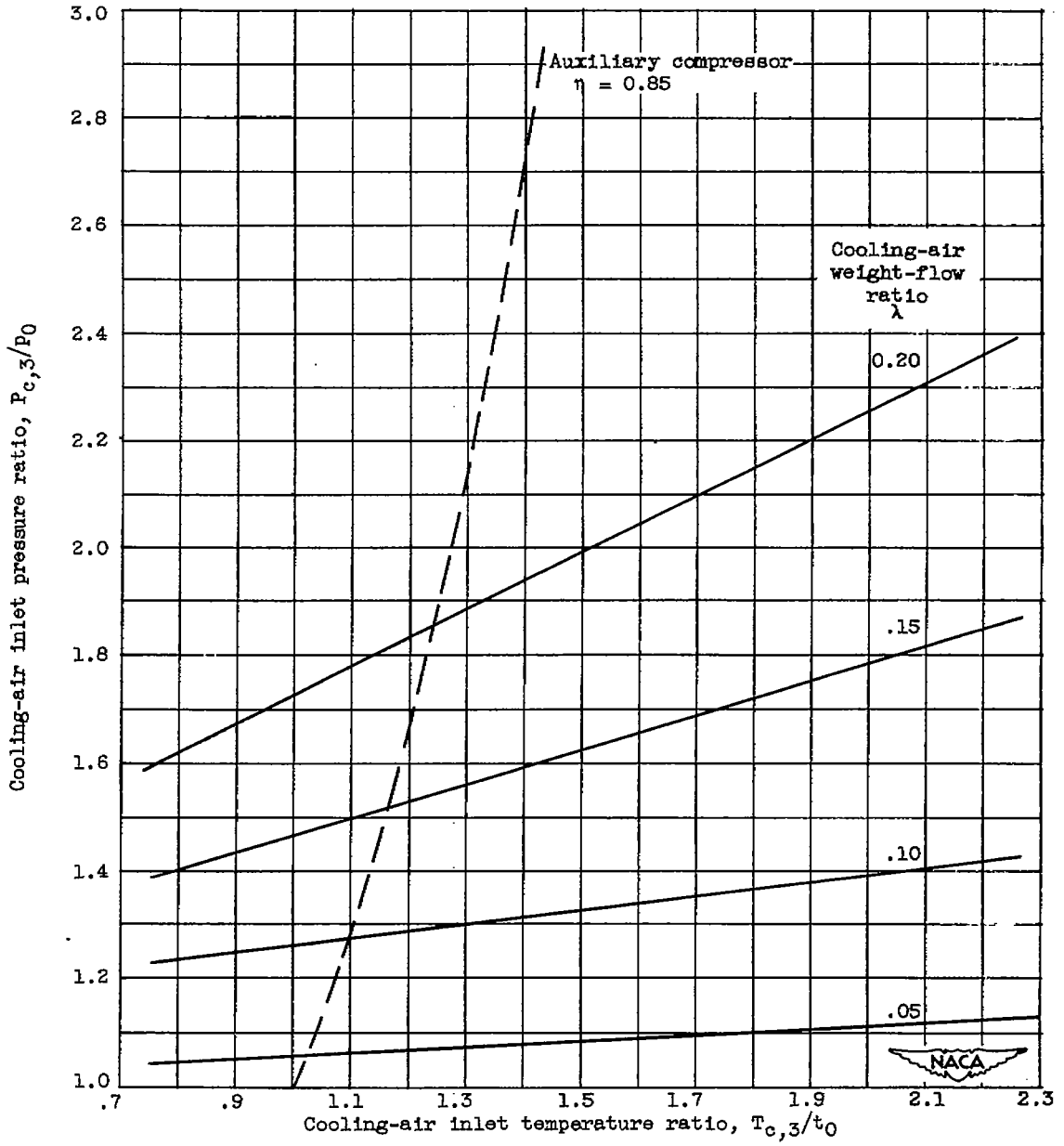

Figure 4. - Cooling-air-passage pumping characteristics at sea-level conditions. Exhaust-gas temperature, 3900° R; flight Mach number, 0.

[redacted]

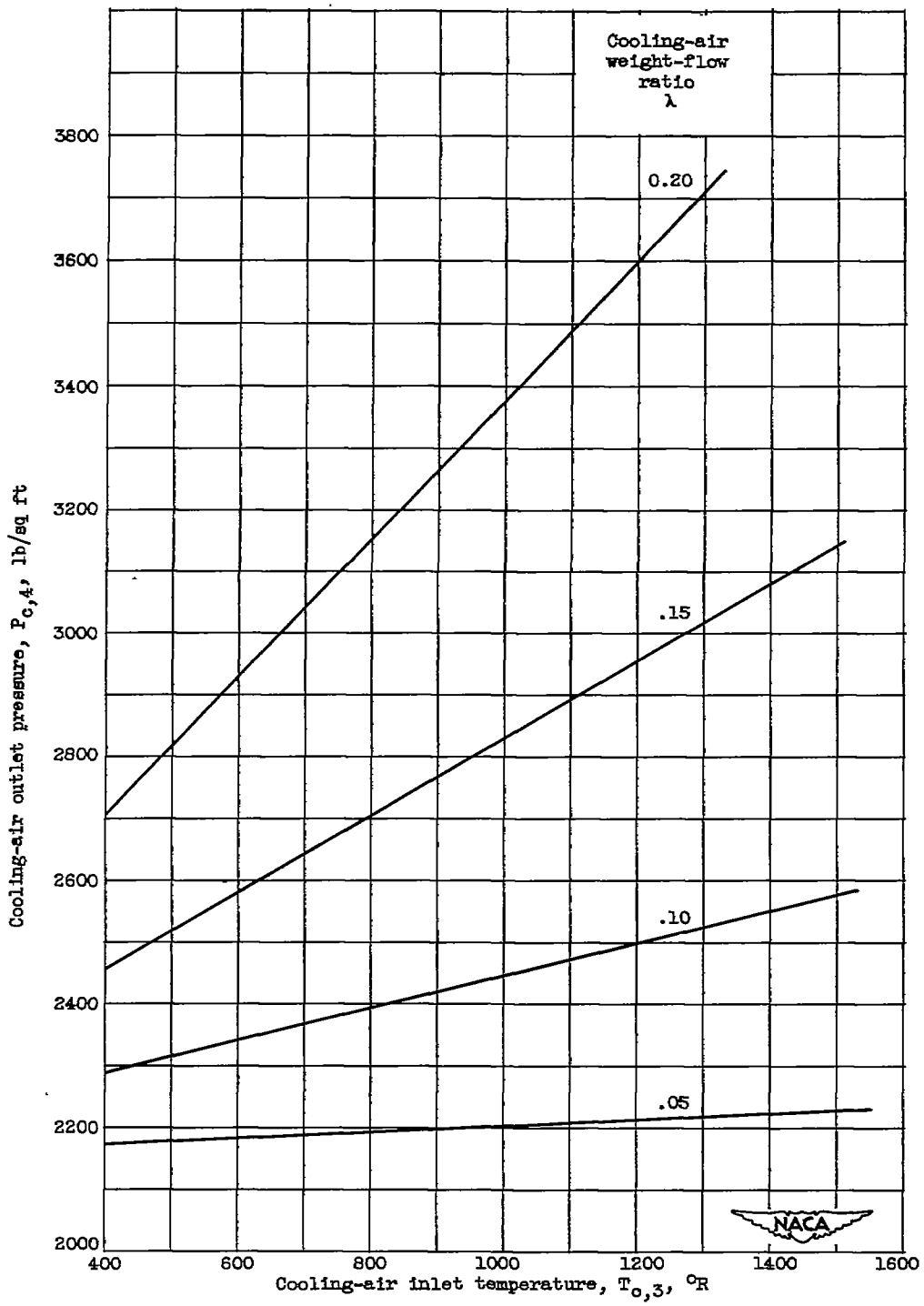

Figure 5. - Cooling-air outlet pressure as a function of cooling-air inlet temperature at sea-level conditions. Exhaust-gas temperature, 3500° R; flight Mach number, 0.

[redacted]

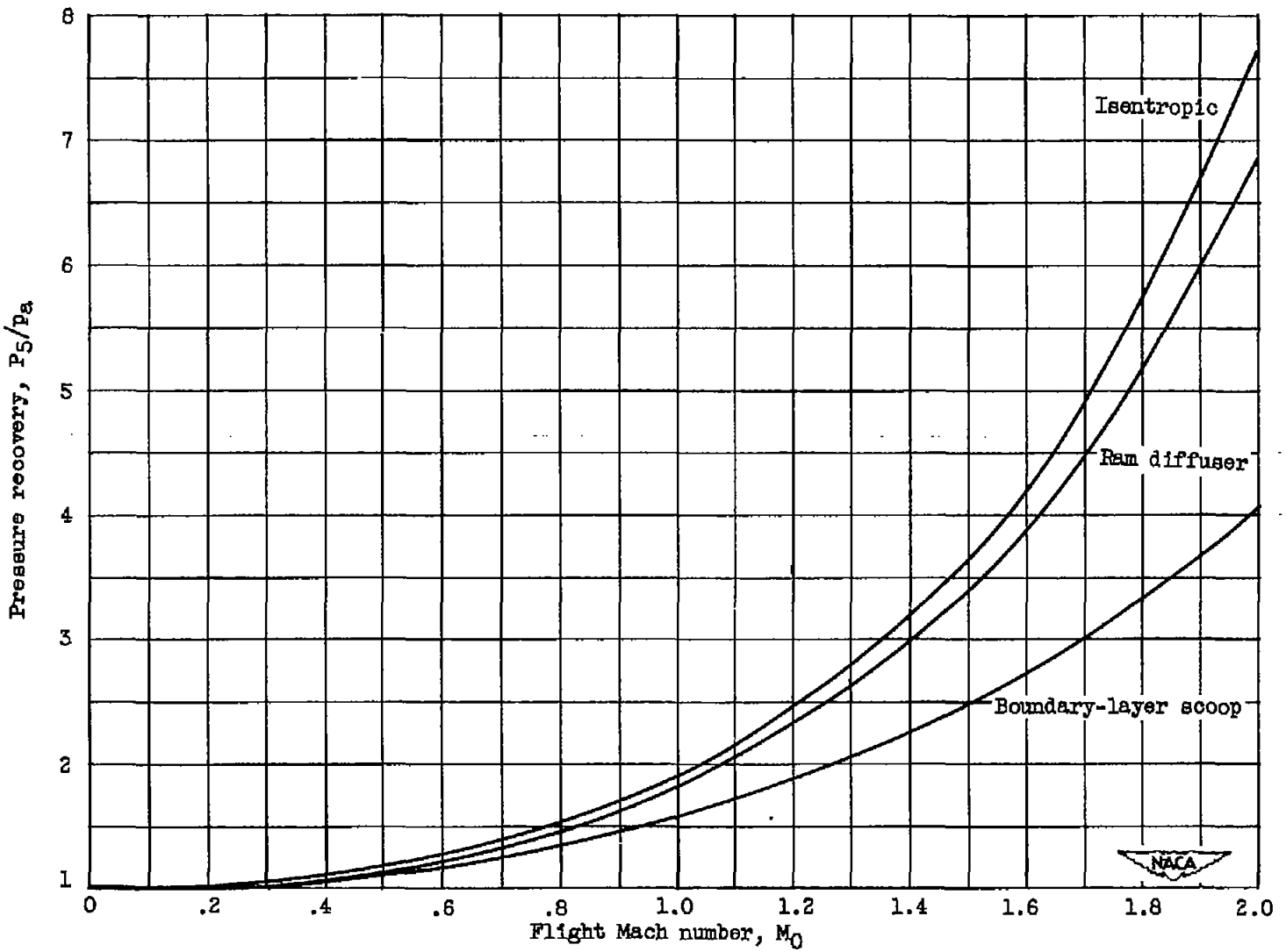

Figure 6. - Pressure recovery as a function of flight Mach number.

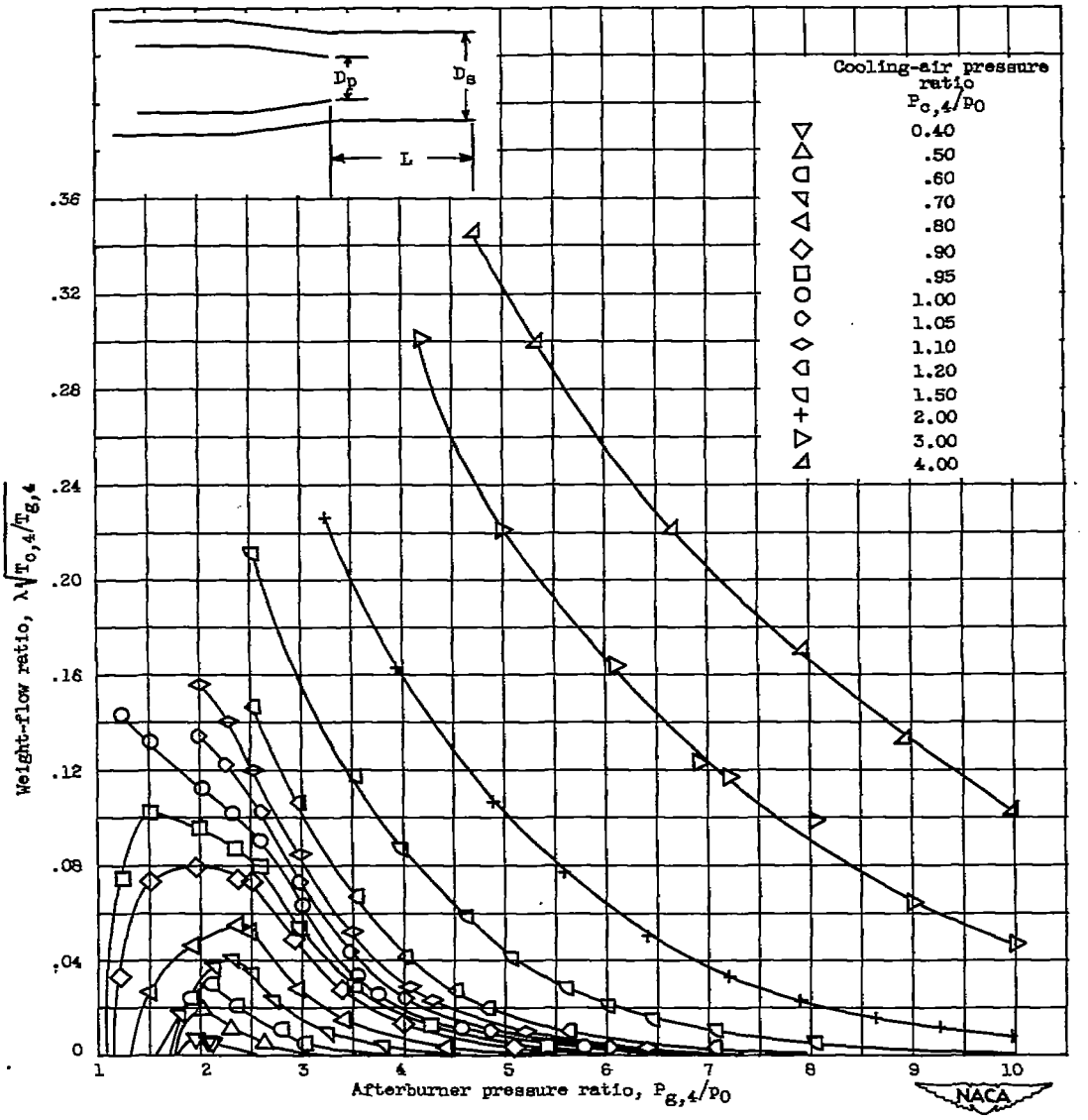

Figure 7. - Typical engine-jet actuated-ejector flow characteristics. Cylindrical shroud; ejector diameter ratio D_s/D_p, 1.21; ejector spacing ratio L/D_p, 1.60.

[redacted]

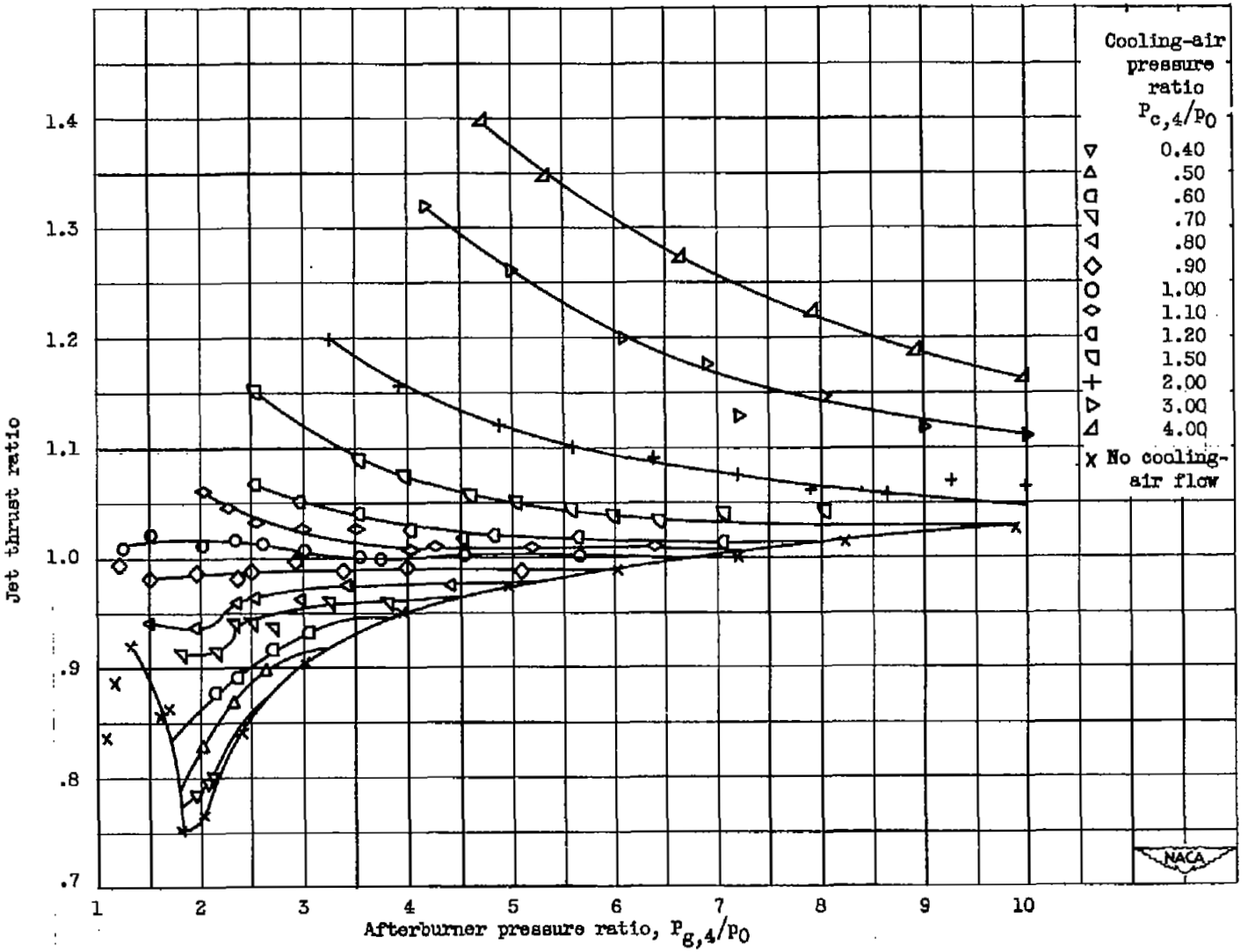

Figure 8. - Typical engine-jet actuated-ejector thrust characteristics. Cylindrical shroud; ejector diameter ratio D_s/D_p, 1.21; ejector spacing ratio L/D_p, 1.60.

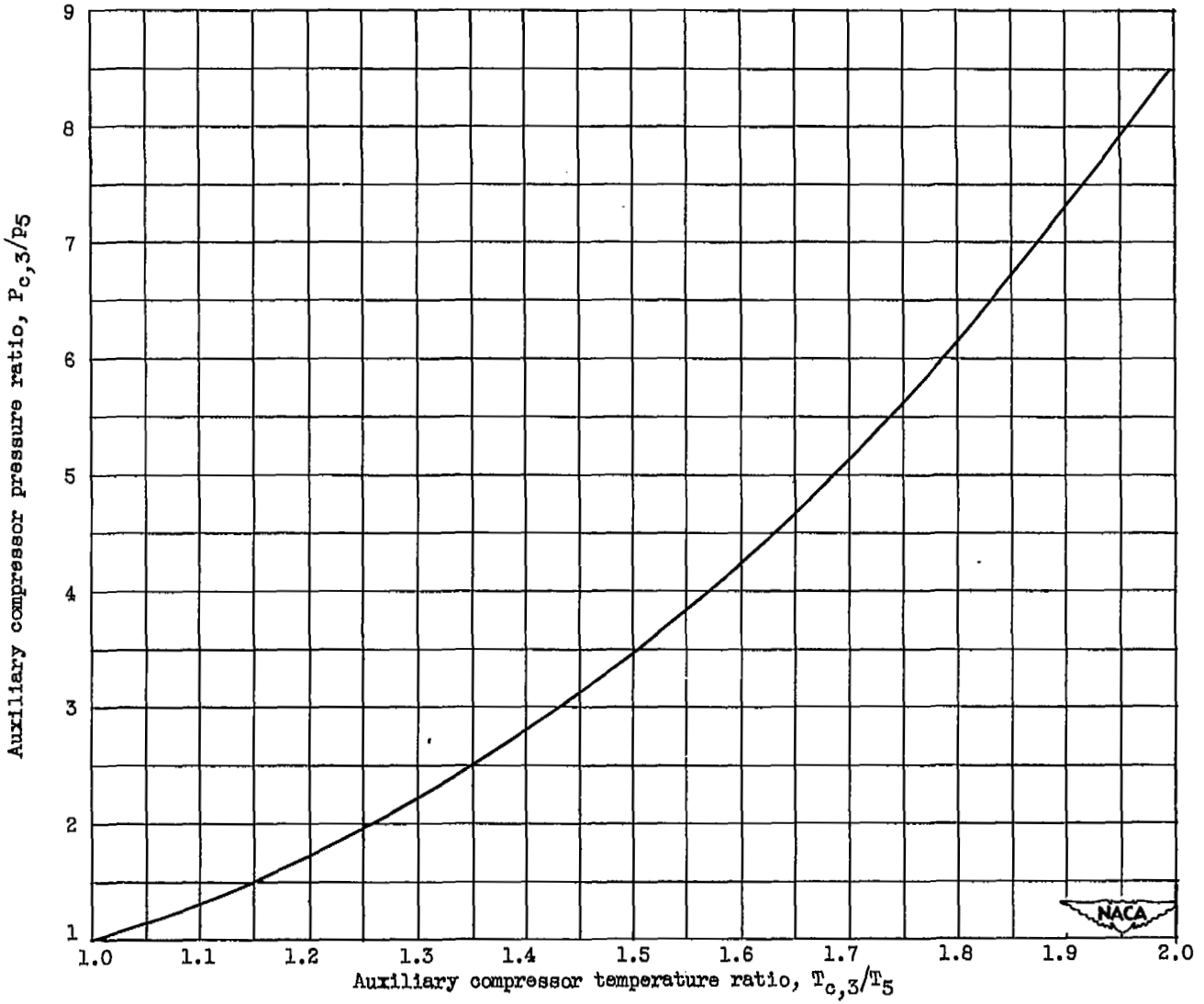

Figure 9. - Pumping characteristics of auxiliary compressor. Compressor efficiency, 85 percent.

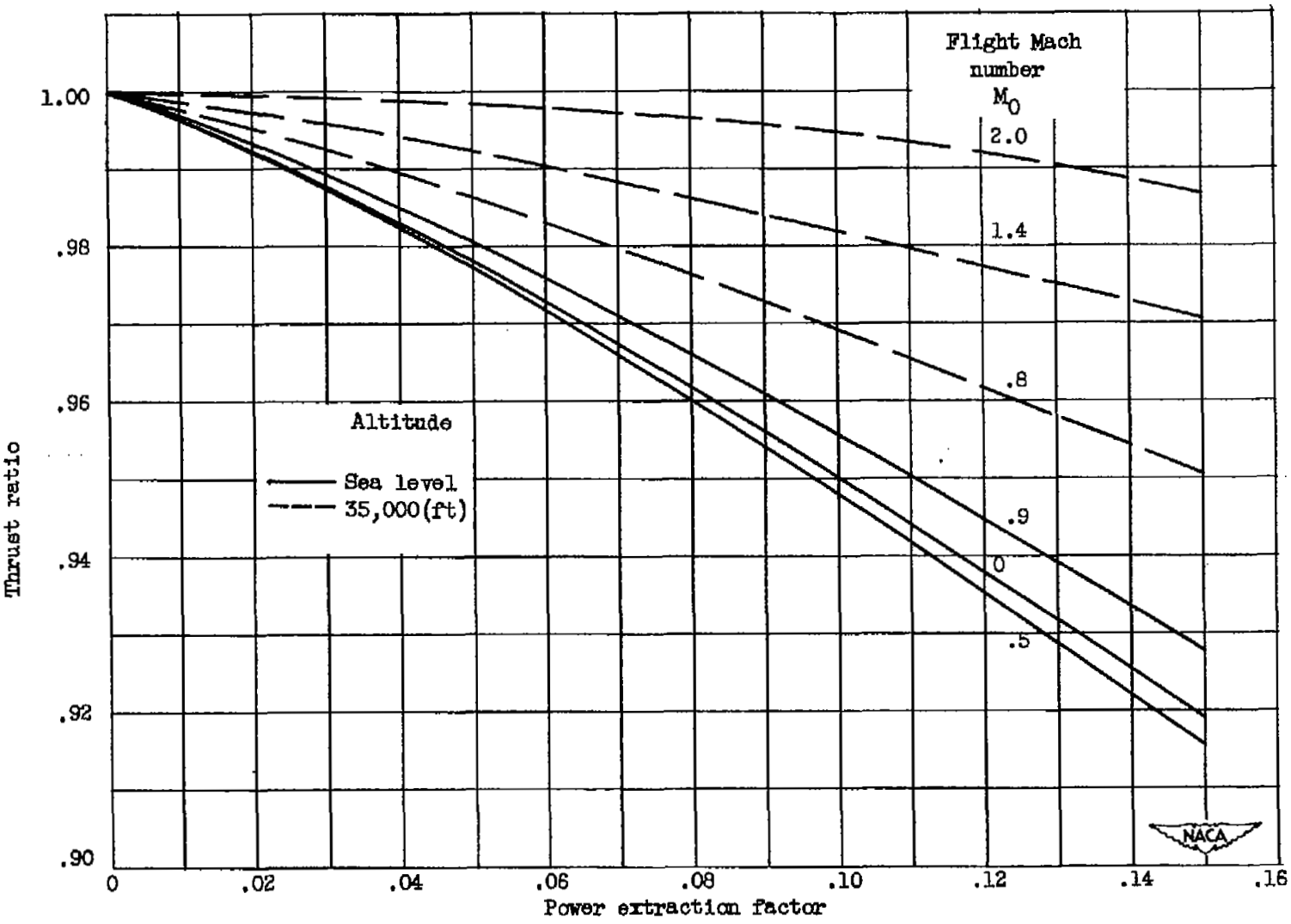

Figure 10. - Thrust ratio as a function of power extraction factor. Exhaust-gas temperature, 3900° R.

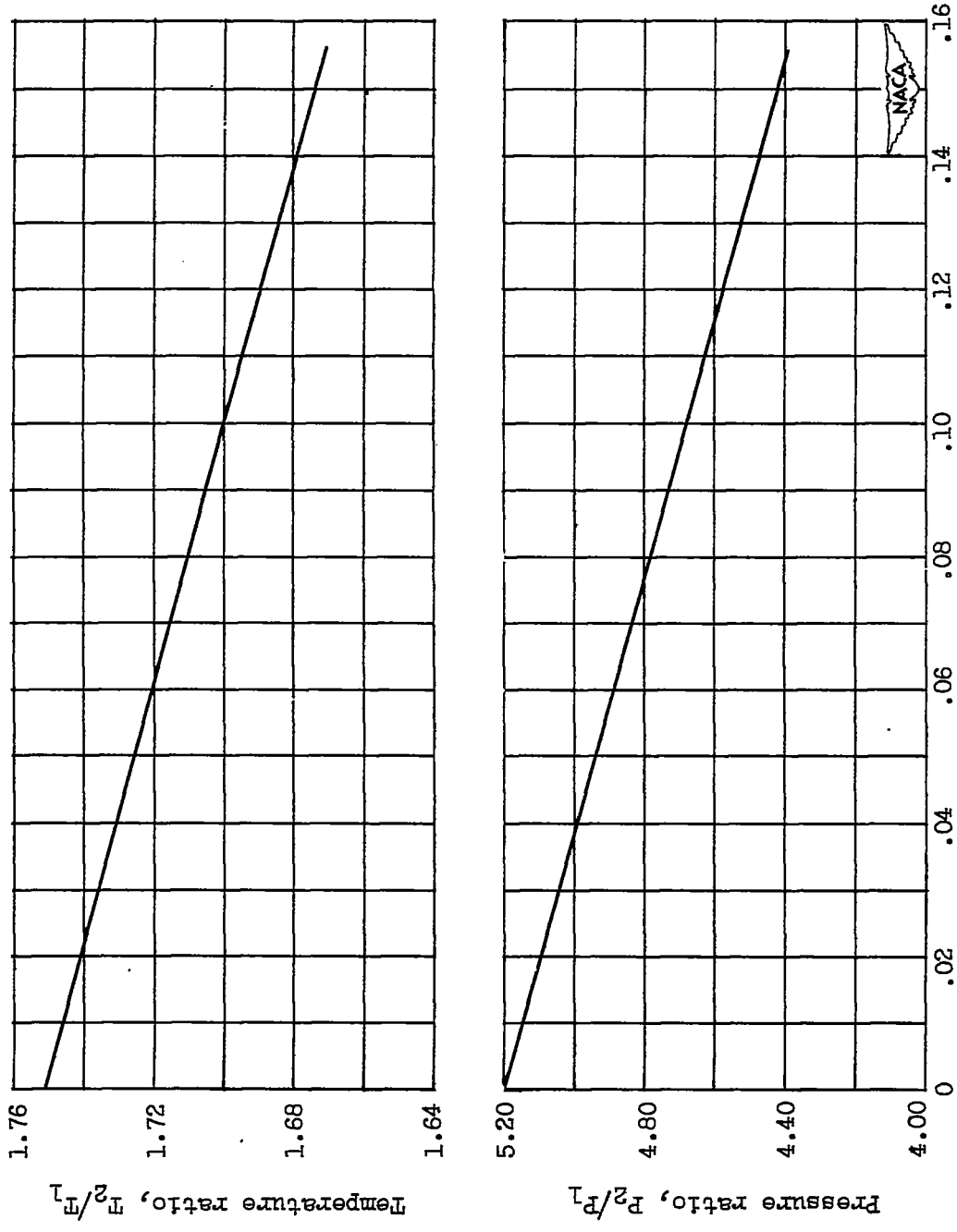

Figure 11. - Compressor temperature and pressure ratios as a function of bleed ratio at sea-level conditions. Flight Mach number, 0.

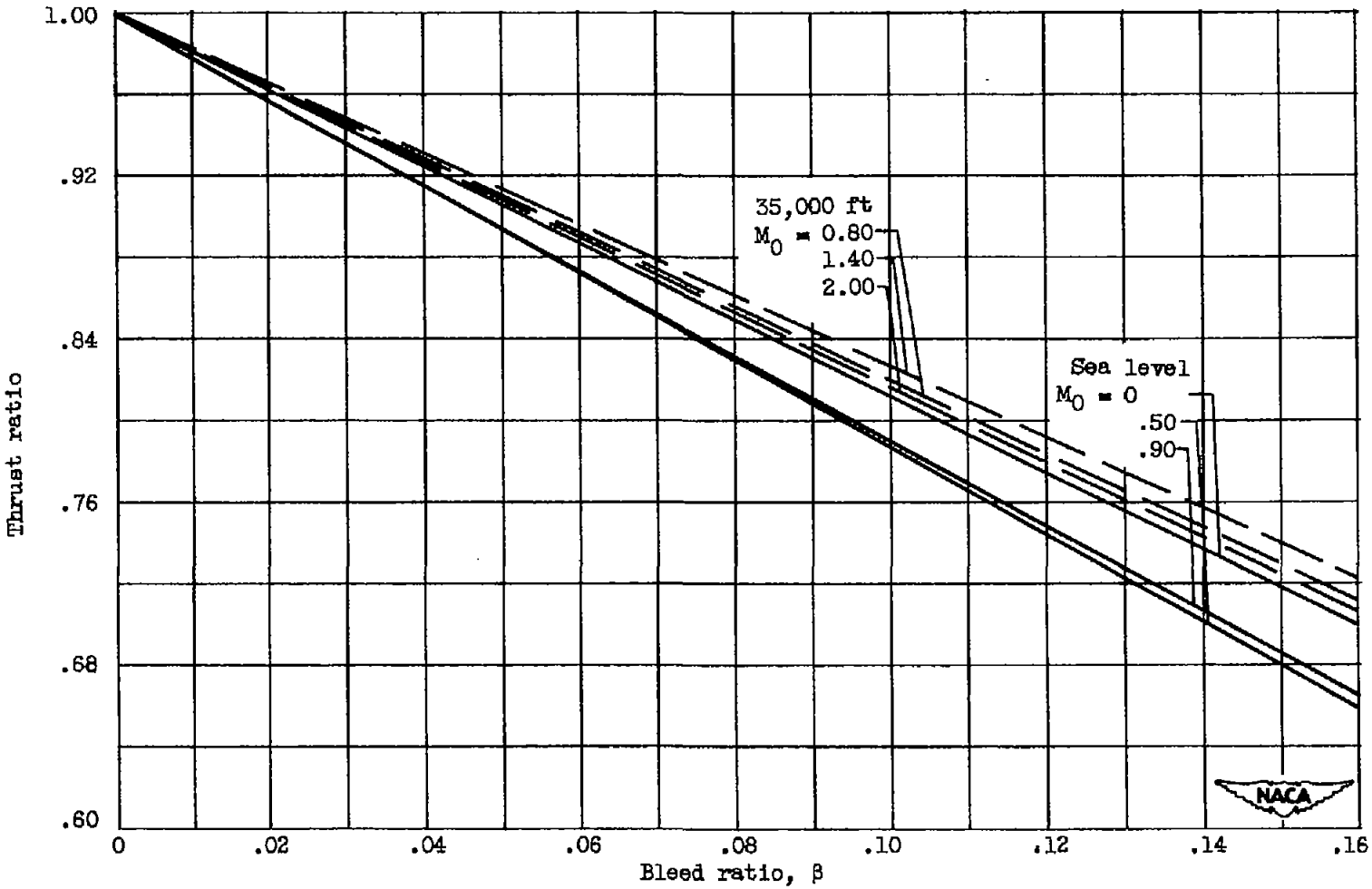

Figure 12. - Thrust ratio as a function of bleed ratio. Exhaust-gas temperature, 3900° R.

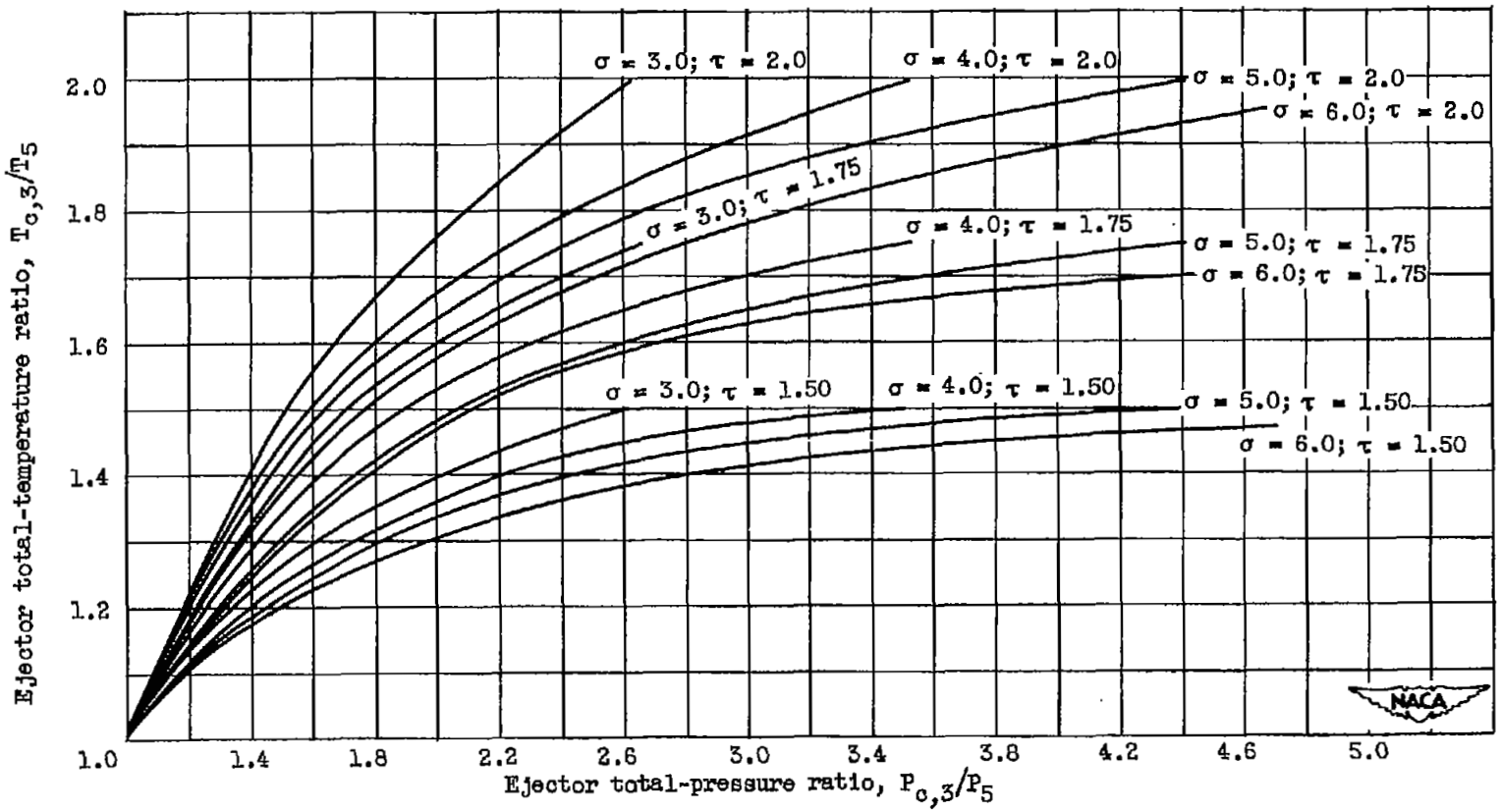

Figure 13. - Pumping characteristics of simple air ejector.

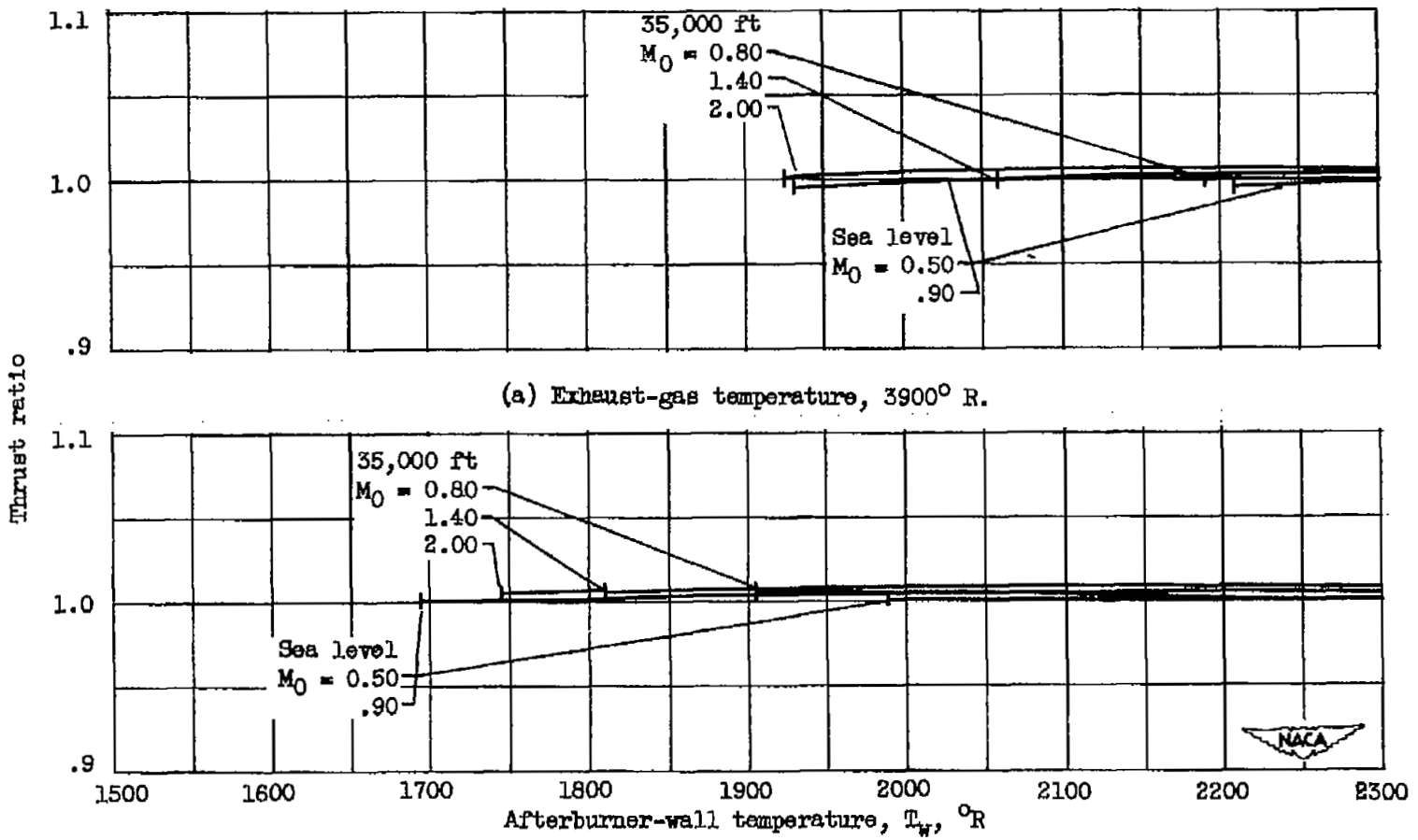

(a) Exhaust-gas temperature, 3900° R.

(b) Exhaust-gas temperature, 3500° R.

Figure 14. - Thrust ratio as a function of afterburner-wall temperature for ram-pressure recovery.

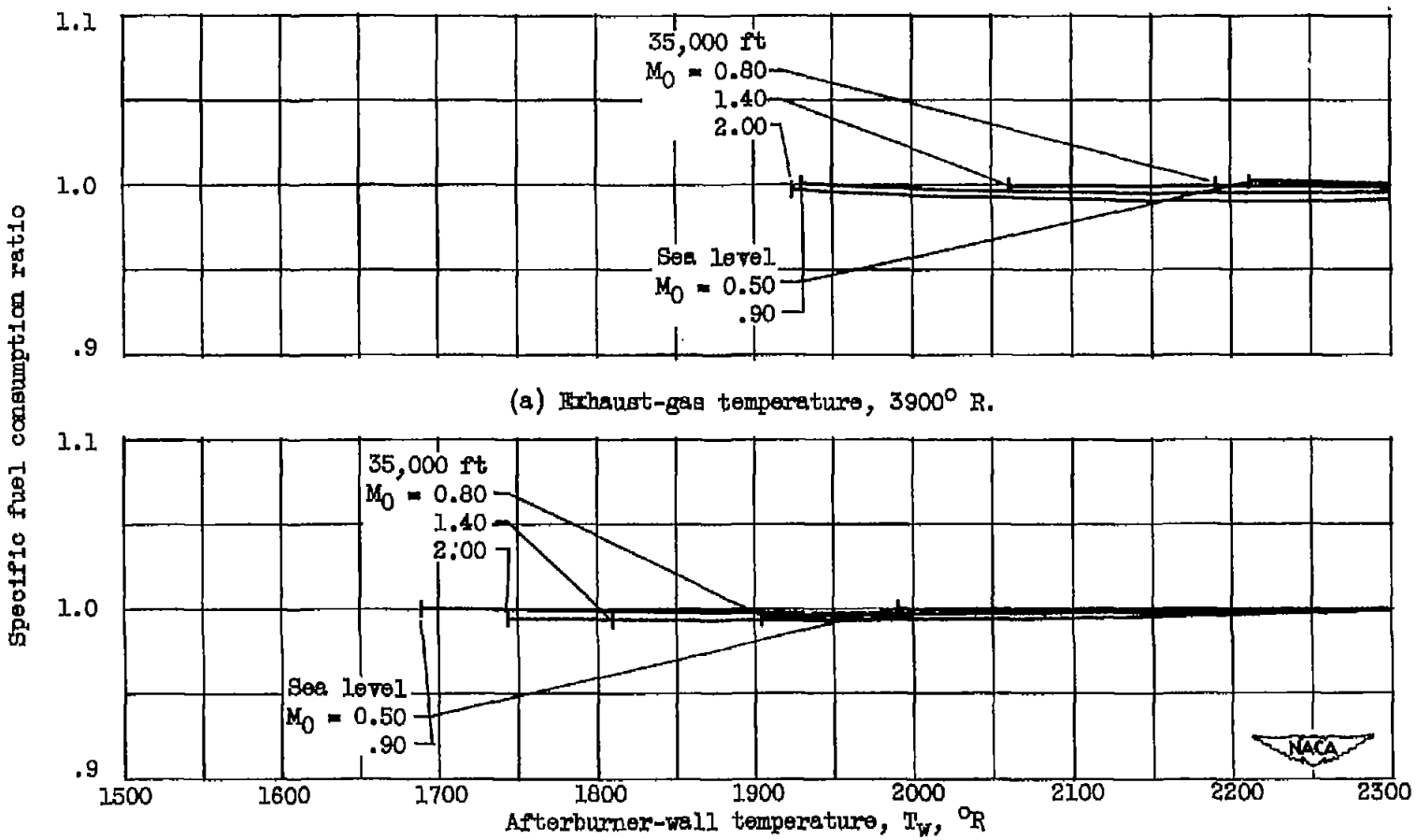

Figure 15. - Specific fuel consumption ratio as a function of afterburner-wall temperature for ram-pressure recovery.

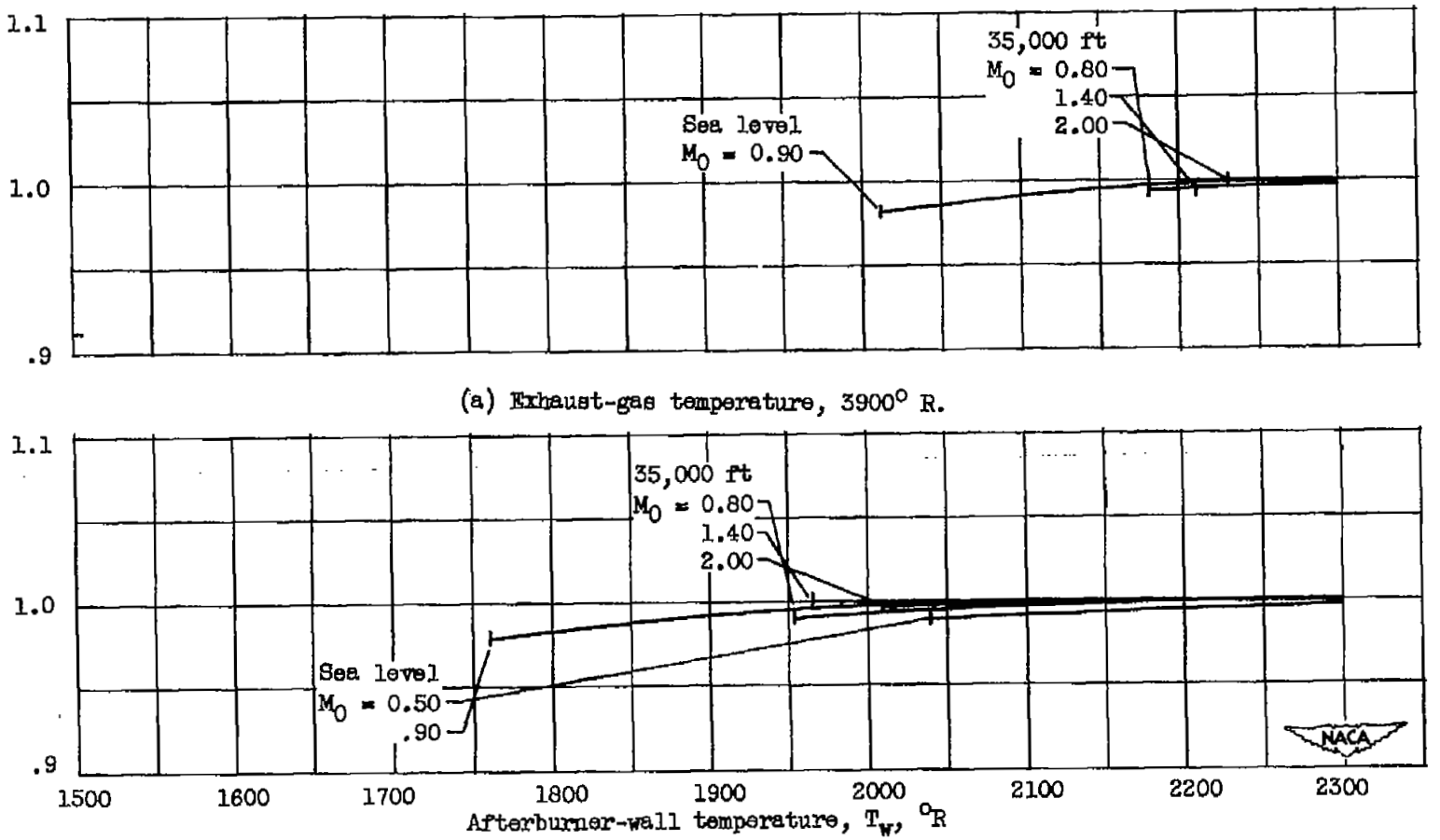

Figure 16. - Thrust ratio as a function of afterburner-wall temperature for boundary-layer pressure recovery.

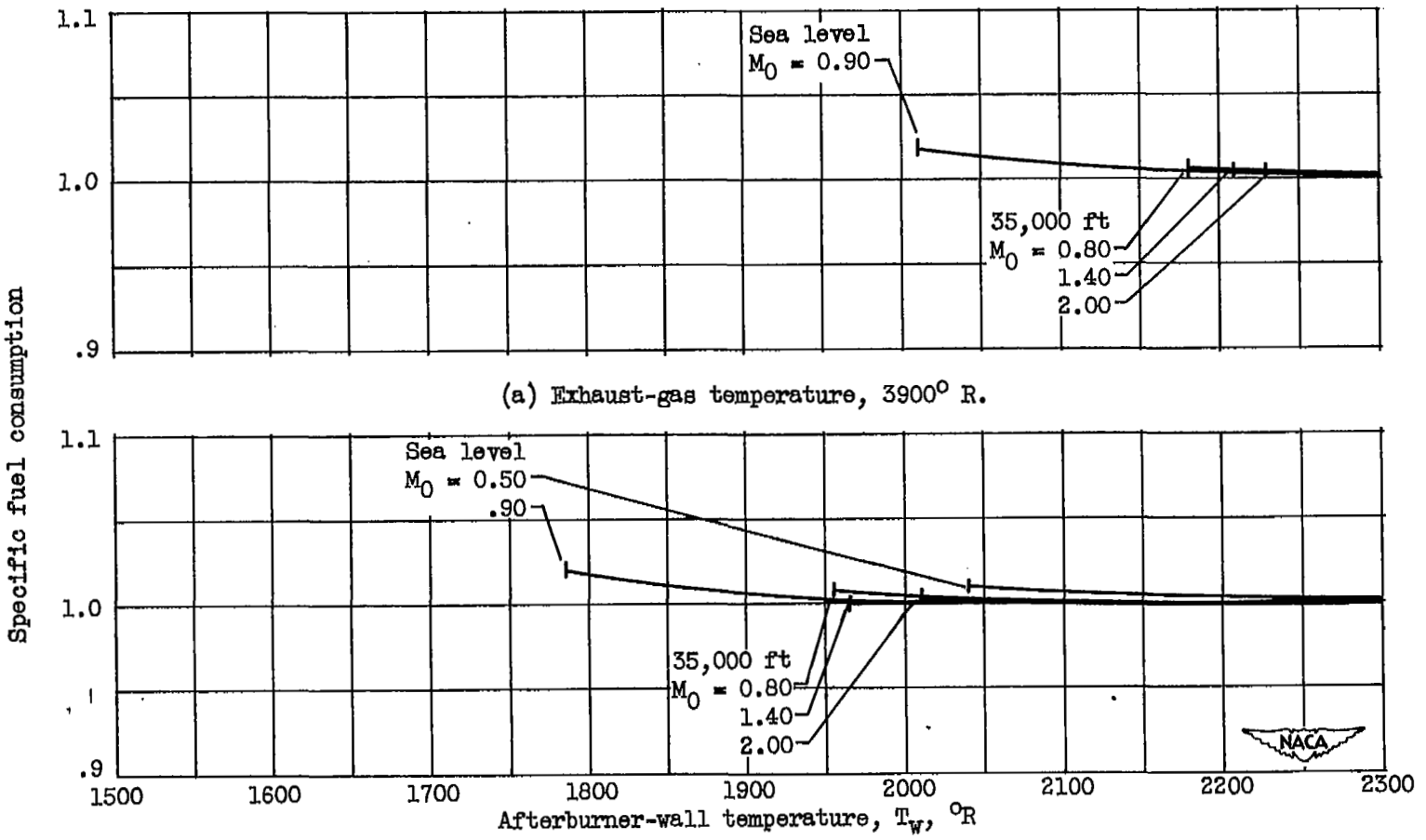

(a) Exhaust-gas temperature, 3900° R.

(b) Exhaust-gas temperature, 3500° R.

Figure 17. - Specific fuel consumption ratio as a function of afterburner-wall temperature for boundary-layer pressure recovery.

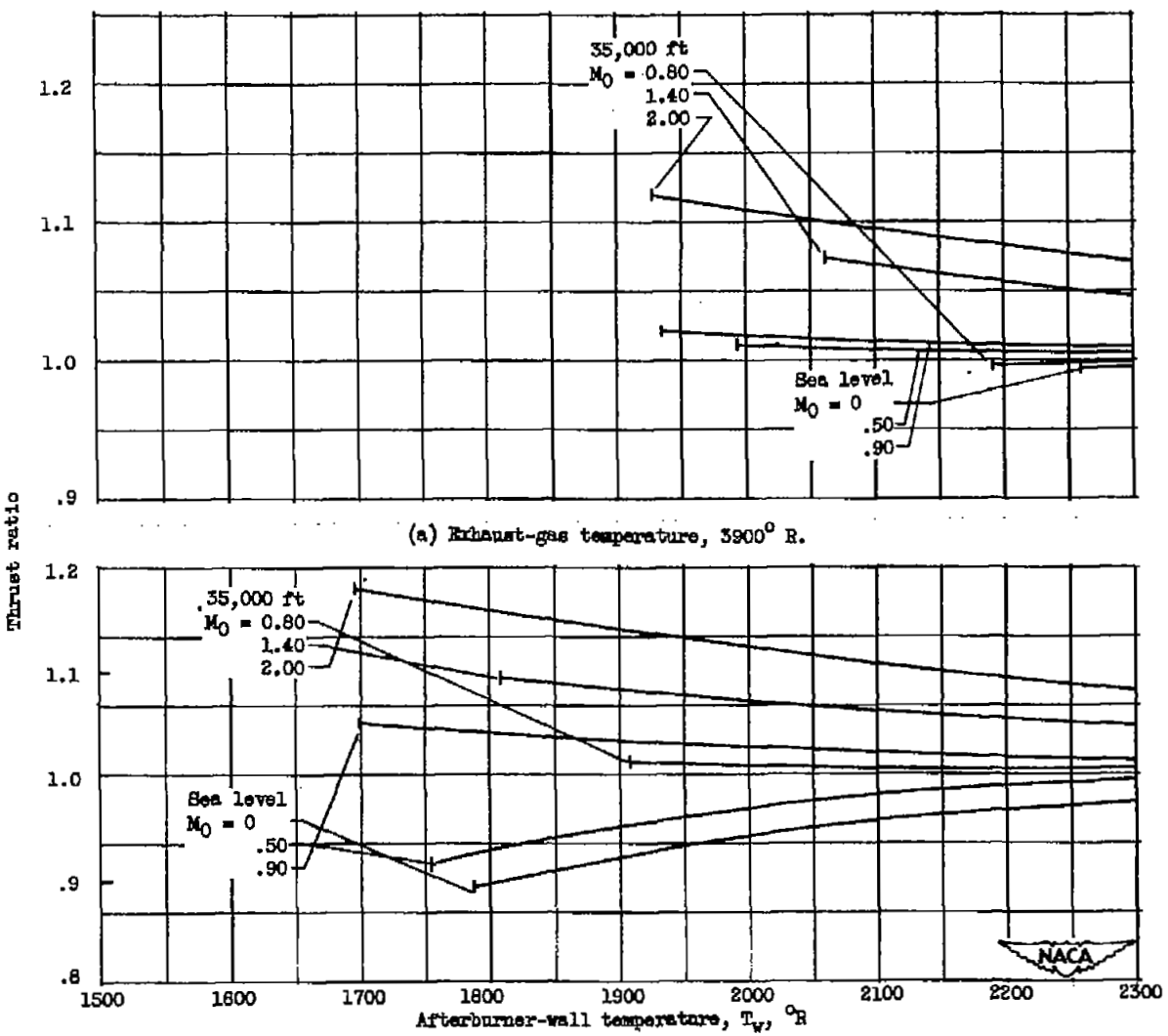

(a) Exhaust-gas temperature, 3900° R.

(b) Exhaust-gas temperature, 3500° R.

Figure 18. - Thrust ratio as a function of afterburner-wall temperature for engine-jet actuated ejector.

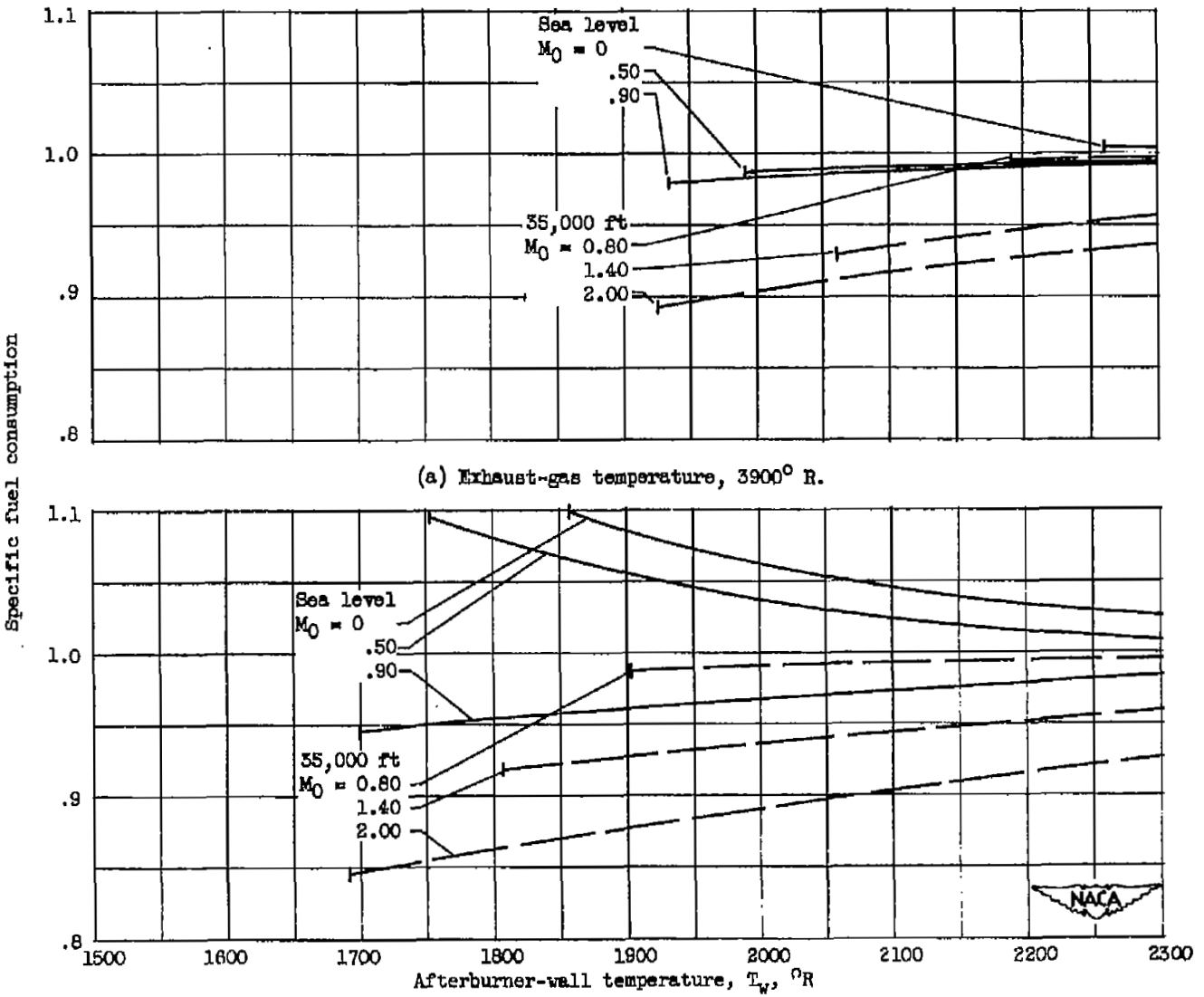

(a) Exhaust-gas temperature, 3900° R.

(b) Exhaust-gas temperature, 3500° R.

Figure 19. - Specific fuel consumption ratio as a function of afterburner-wall temperature for engine-jet actuated ejector.

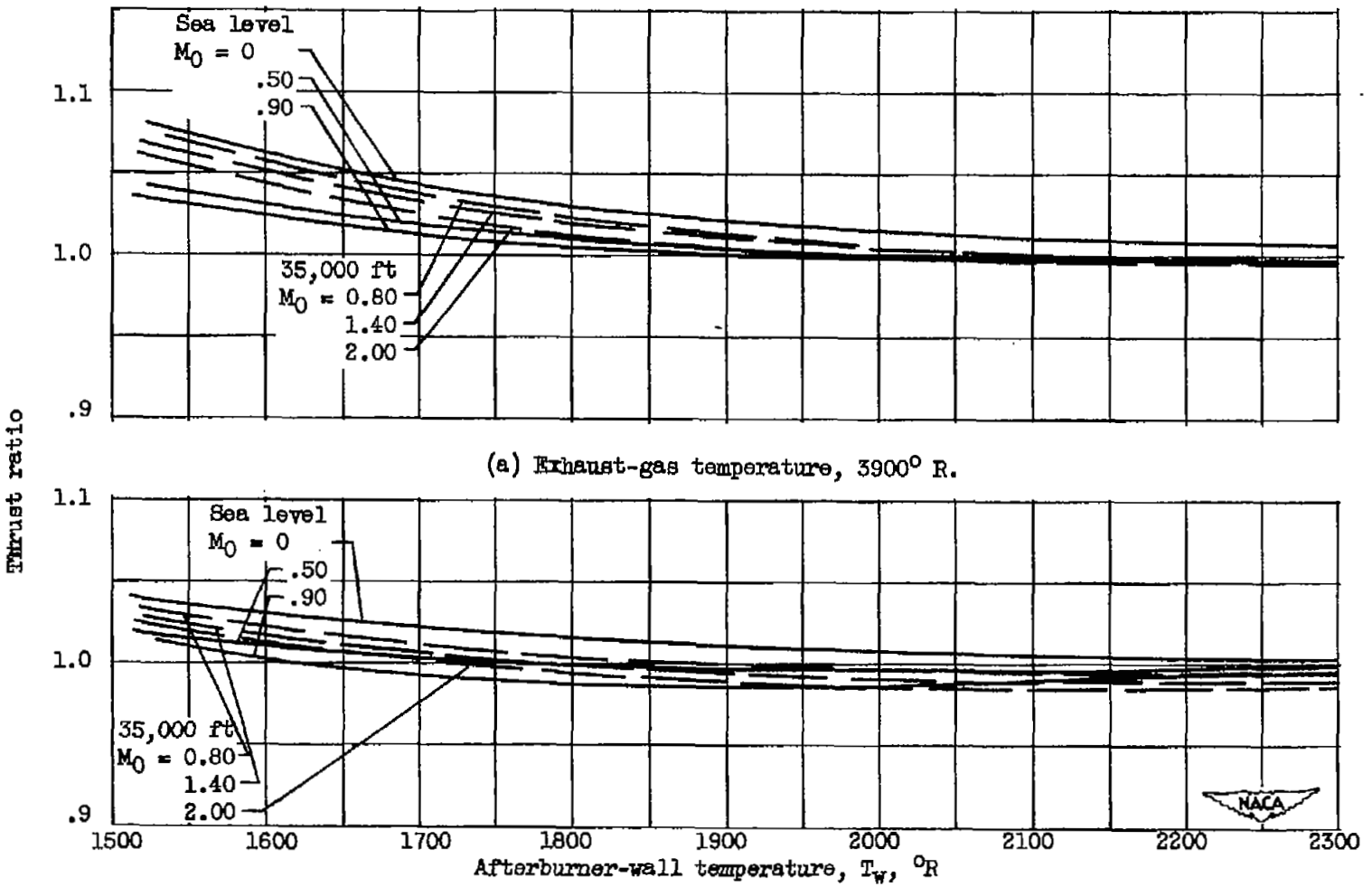

Figure 20. - Thrust ratio as a function of afterburner-wall temperature for auxiliary compressor.

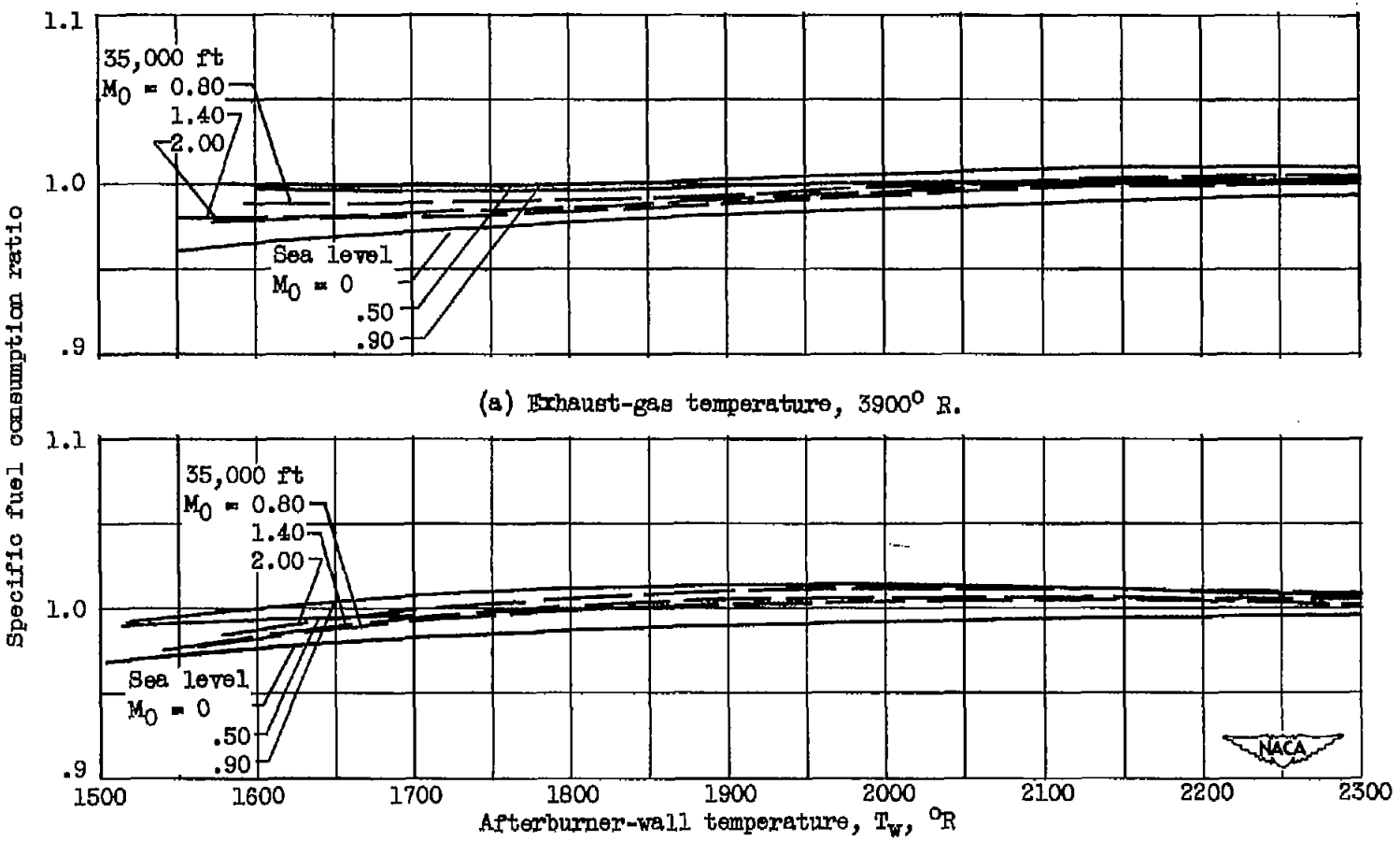

Figure 21. - Specific fuel consumption ratio as a function of afterburner-wall temperature for auxiliary compressor.

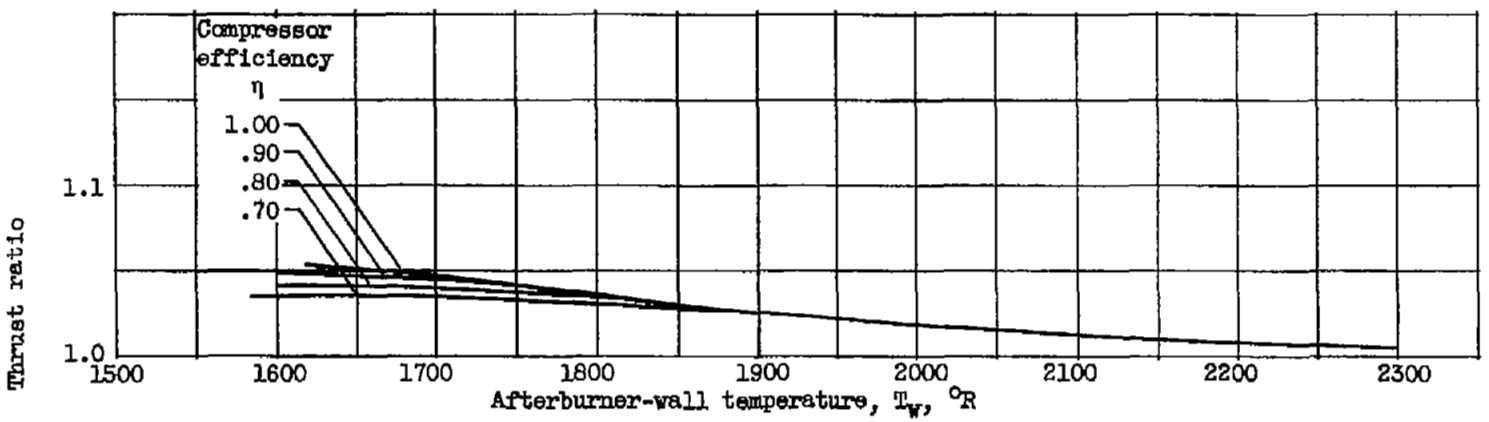

Figure 22. - Thrust ratio as a function of afterburner-wall temperature for auxiliary compressors of various efficiencies at sea-level conditions. Flight Mach number, 0; exhaust-gas temperature, 3900° R.

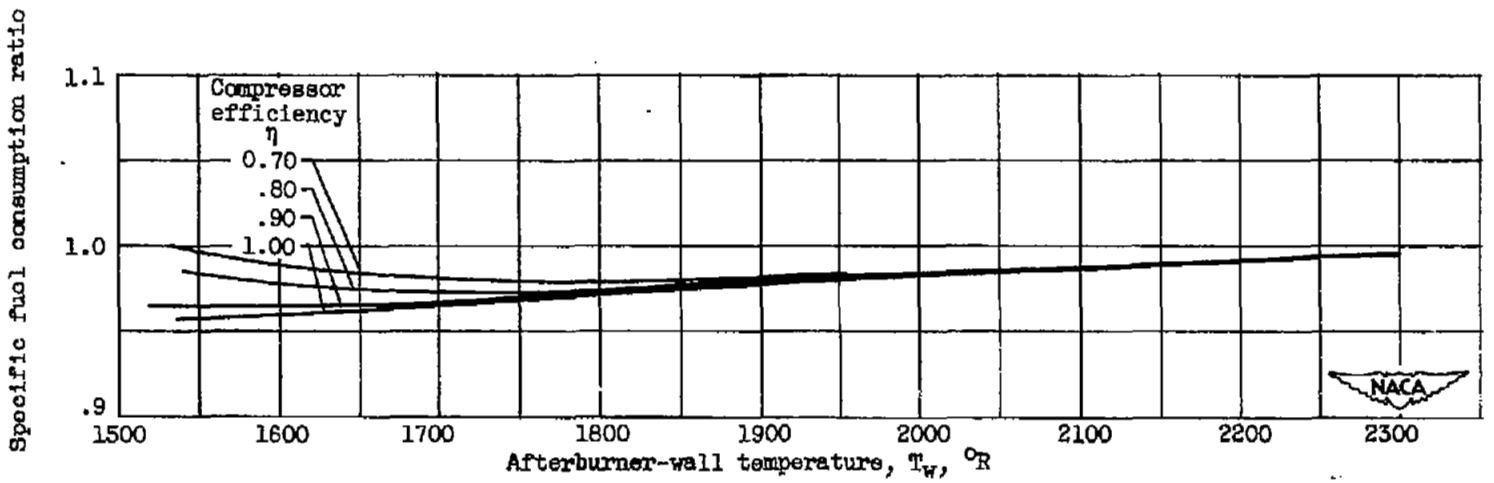

Figure 23. - Specific fuel consumption ratio as a function of afterburner-wall temperature for auxiliary compressors of various efficiencies at sea-level conditions. Flight Mach number, 0; exhaust-gas temperature, 3900° R.

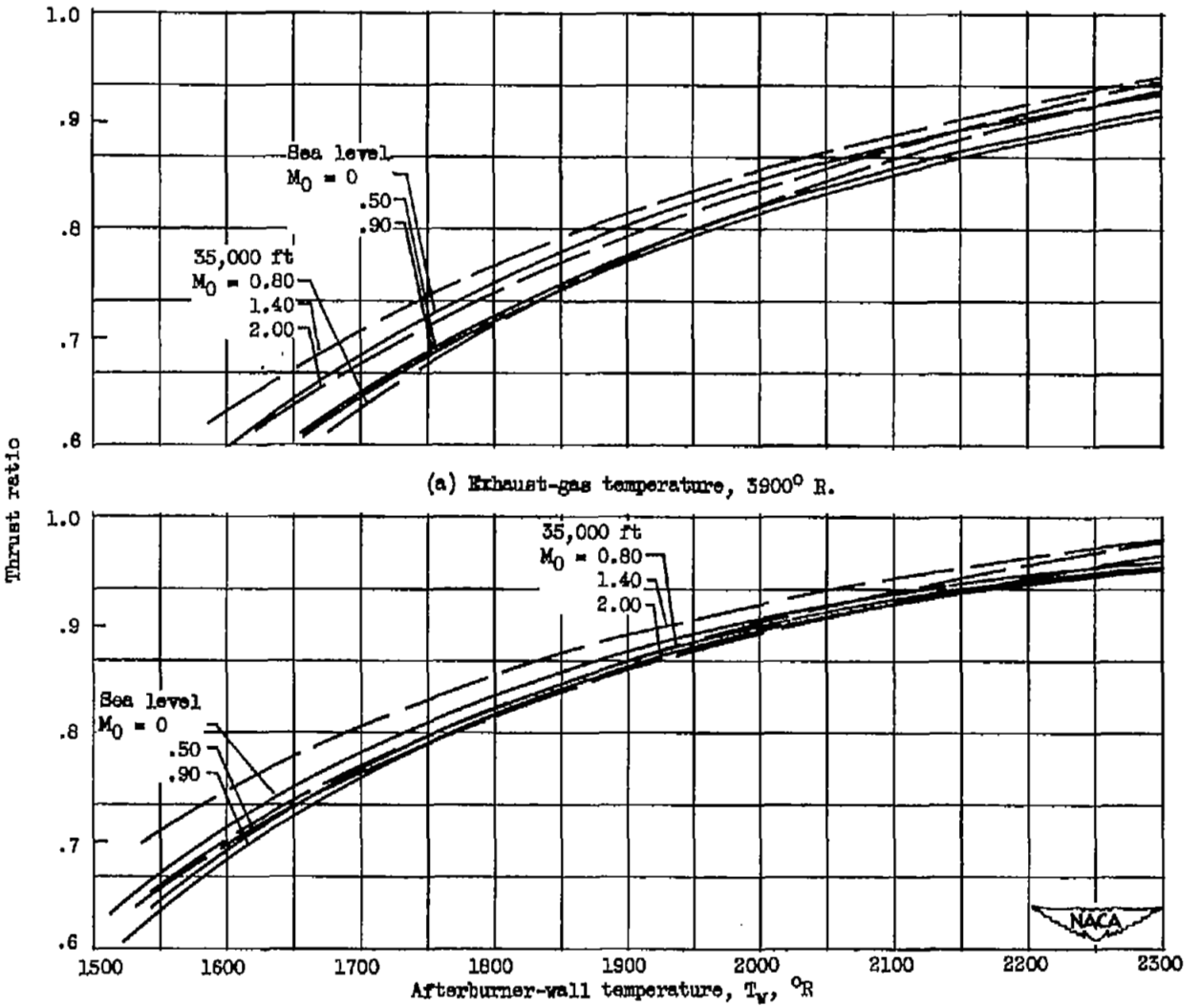

Figure 24. - Thrust ratio as a function of afterburner-wall temperature for compressor air-bleed cooling.

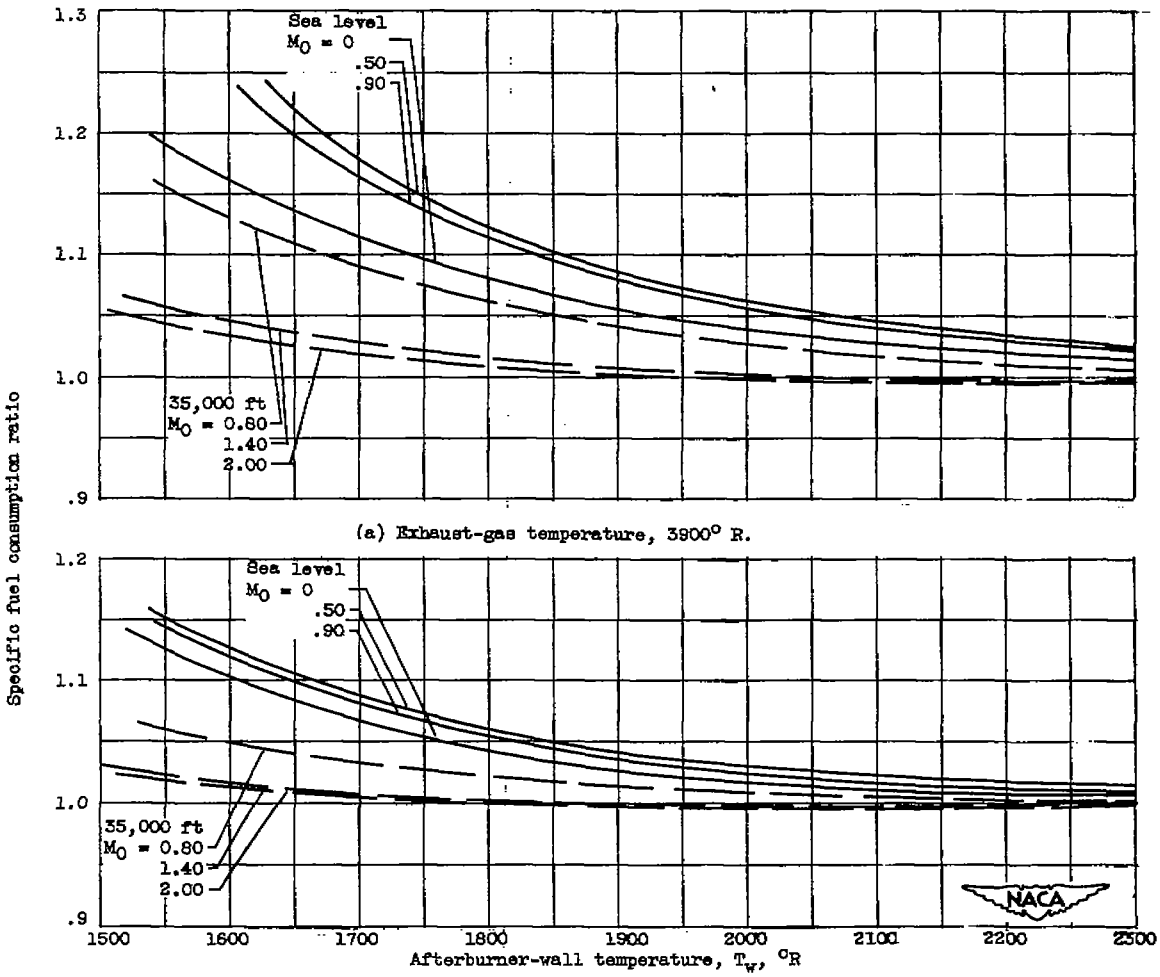

(a) Exhaust-gas temperature, 3900° R.

(b) Exhaust-gas temperature, 3500° R.

Figure 25. - Specific fuel consumption ratio as a function of afterburner-wall temperature for compressor air-bleed cooling.

[redacted]

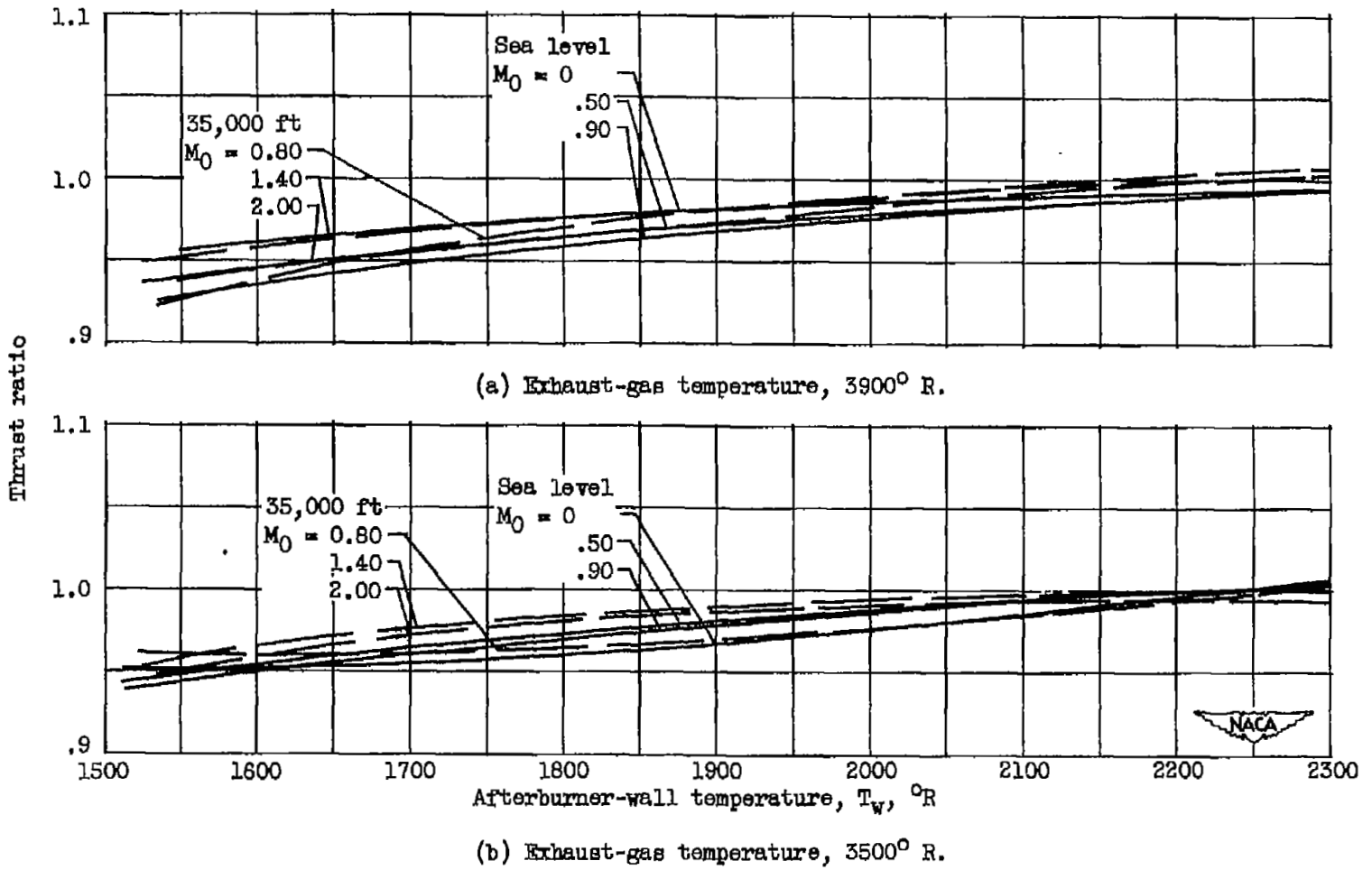

(a) Exhaust-gas temperature, 3900° R.

(b) Exhaust-gas temperature, 3500° R.

Figure 26. - Thrust ratio as a function of afterburner-wall temperature for compressor bleed-air actuated ejector.

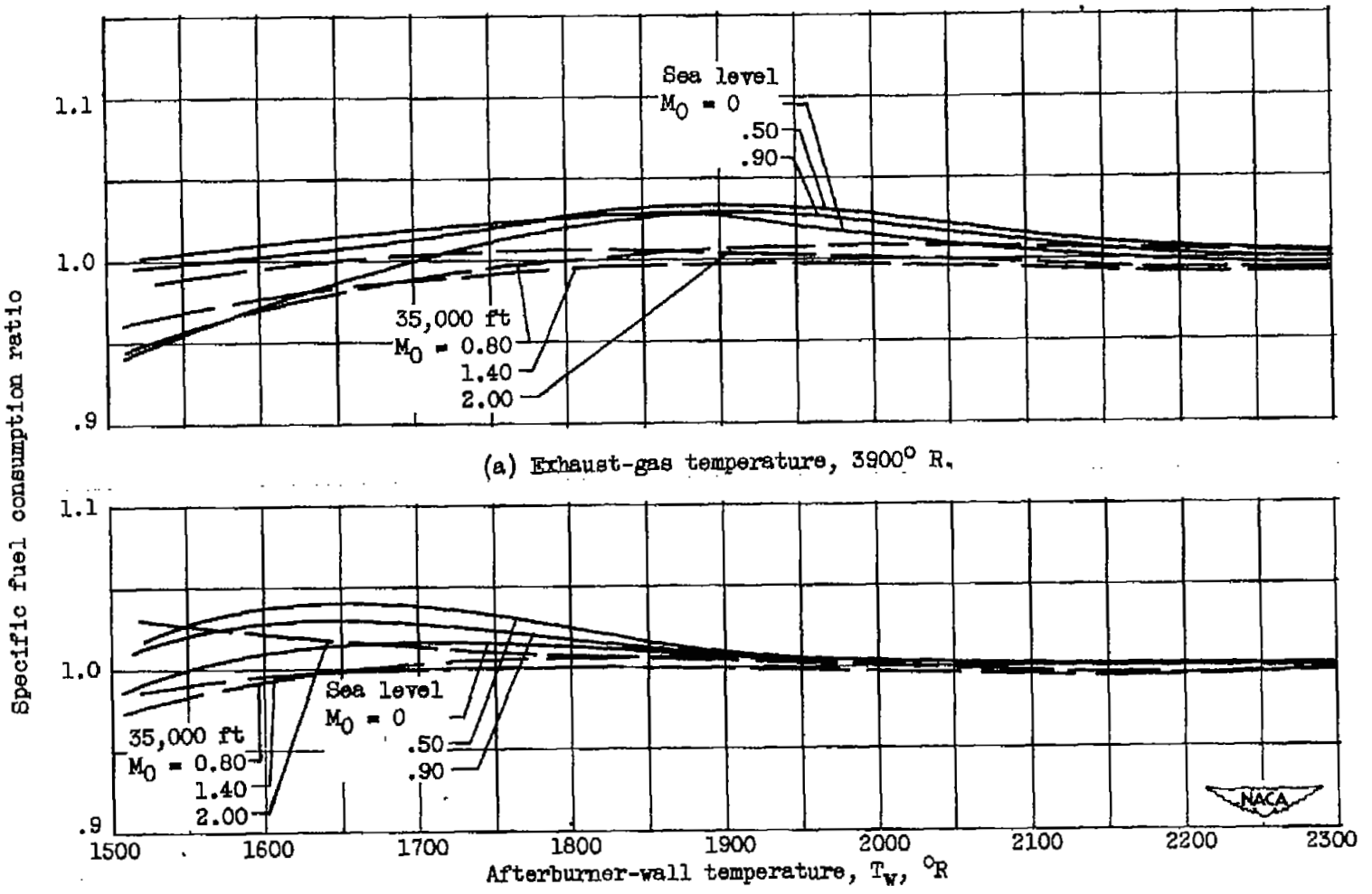

Figure 27. - Specific fuel consumption ratio as a function of afterburner-wall temperature for compressor bleed-air actuated ejector.

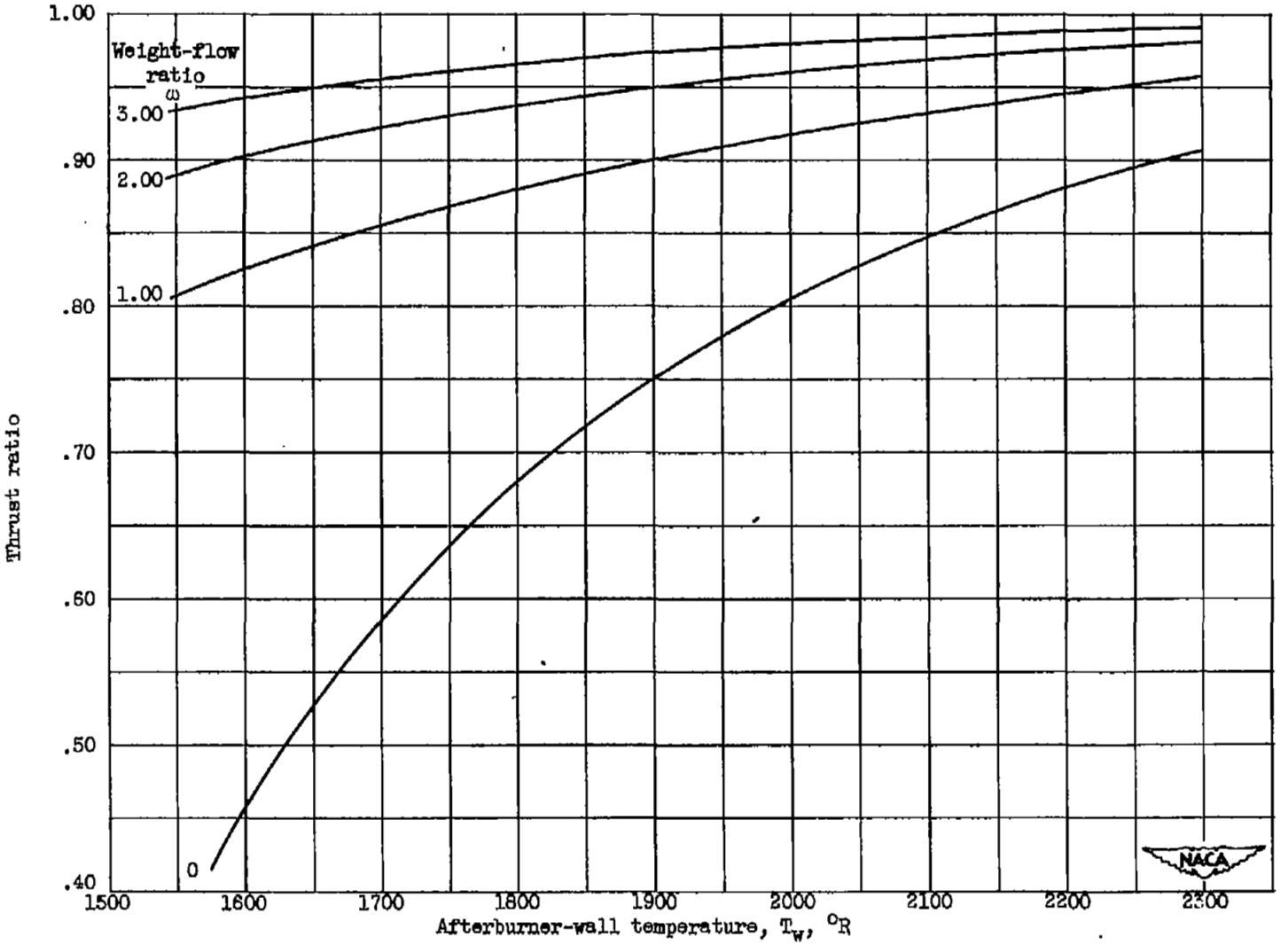

Figure 28. - Effect on thrust ratio of various weight-flow ratios for compressor bleed-air actuated ejector at sea-level conditions. Flight Mach number, 0; exhaust-gas temperature, 3900° R.

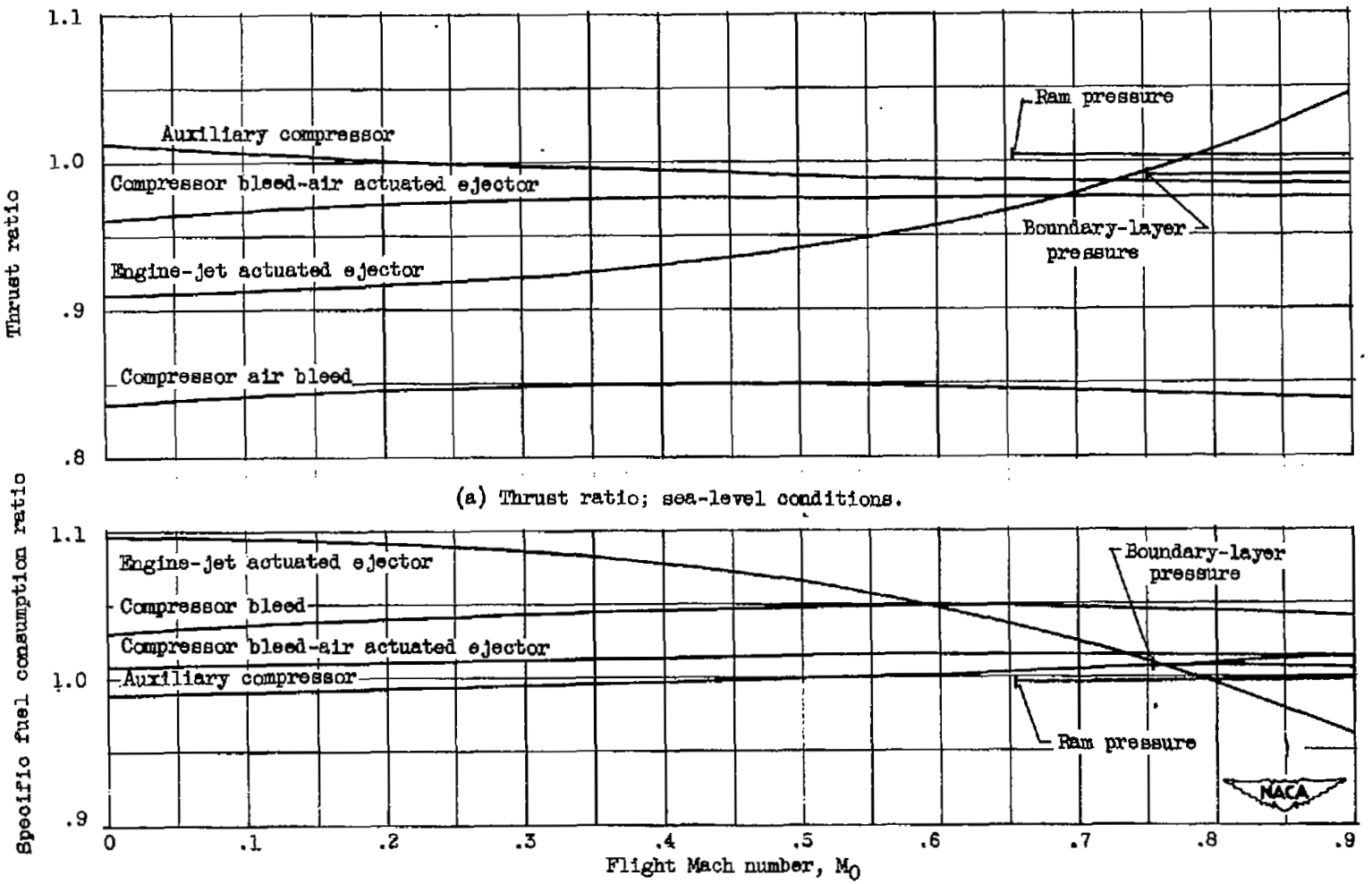

(a) Thrust ratio; sea-level conditions.

(b) Specific fuel consumption ratio; sea-level conditions.

Figure 29. - Comparison of thrust ratio and specific fuel consumption ratio with various cooling schemes. Afterburner-wall temperature, 1860° R; exhaust-gas temperature, 3500° R.

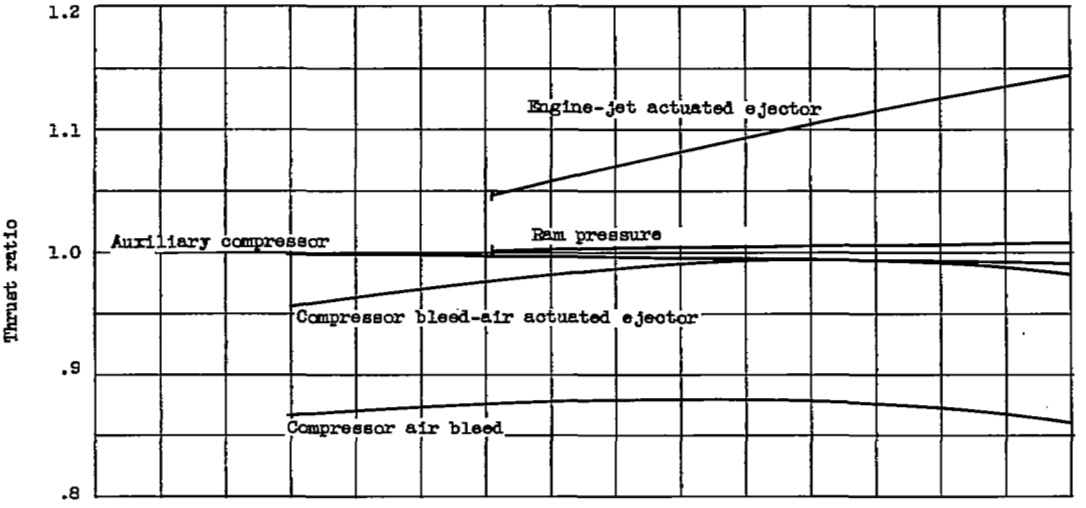

(c) Thrust ratio; altitude, 35,000 feet.

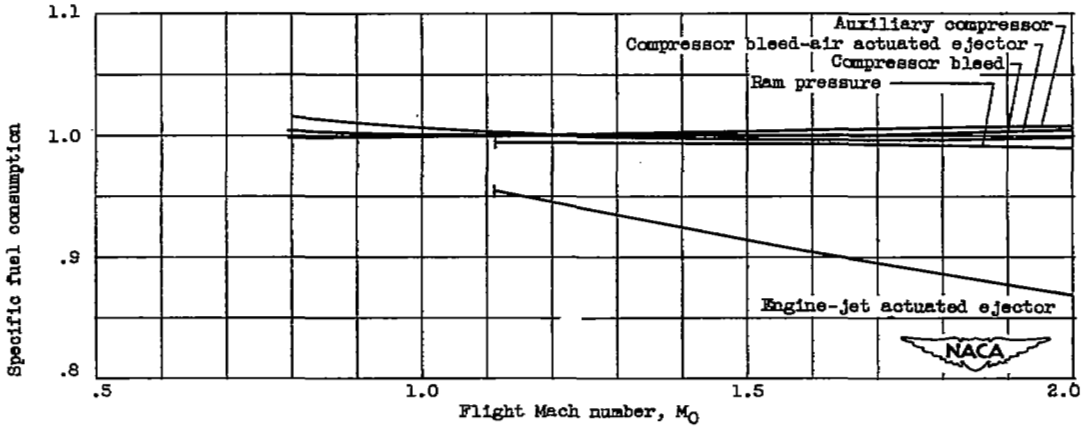

(d) Specific fuel consumption ratio; altitude, 35,000 feet.

Figure 29. - Concluded. Comparison of thrust ratio and specific fuel consumption ratio with various cooling schemes. Afterburner-wall temperature, 1860° R; exhaust-gas temperature, 3500° R.

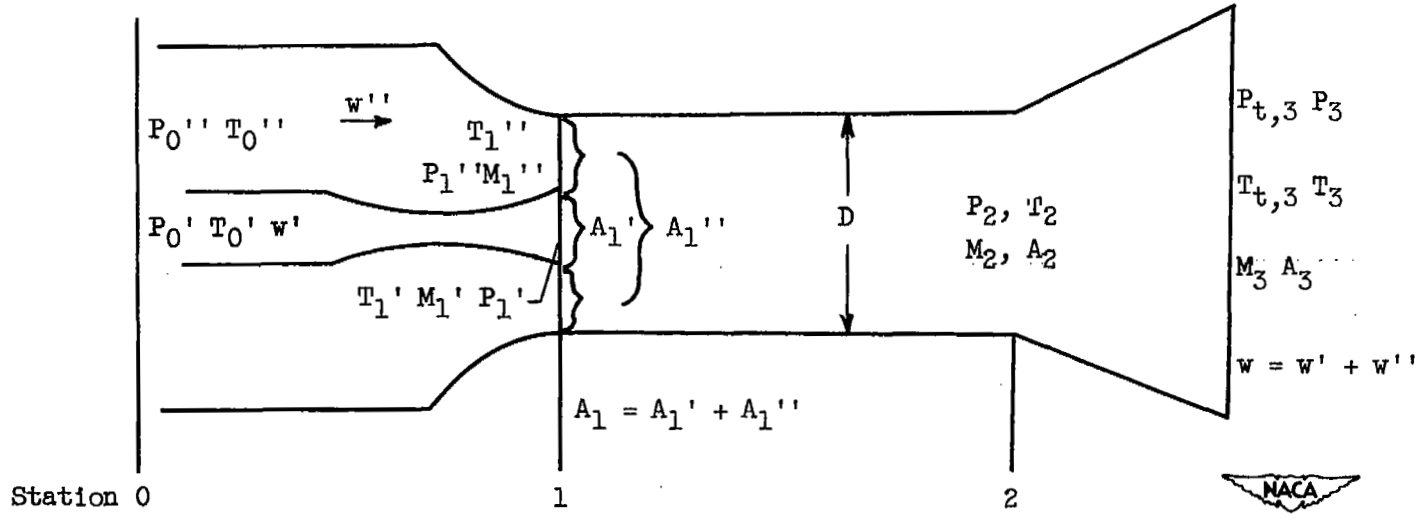

Figure 30. - Schematic diagram of compressor bleed-air ejector.

NACA-Langley - 2-2-53 - 400

[redacted]

[redacted]